Discovery of long-chain salicylketoxime derivatives as monoacylglycerol lipase (MAGL) inhibitors

Giulia Bononi [a], Carlotta Granchi [a,], Margherita Lapillo [a], Massimiliano Giannotti [a], Daniela Nieri [b], Serena Fortunato [a], Maguie el Boustani [c, d], Isabella Caligiuri [c], Giulio Poli [a], Kathryn E. Carlson [e], Sung Hoon Kim [e], Marco Macchia [a], Adriano Martinelli [a], Flavio Rizzolio [c, f], Andrea Chicca [b], John A. Katzenellenbogen [e], Filippo Minutolo [a], Tiziano Tuccinardi [a]*

[a] Department of Pharmacy, University of Pisa, Via Bonanno 6, 56126 Pisa, Italy.

[b] Institute of Biochemistry and Molecular Medicine, NCCR TransCure, University of Bern, CH-3012 Bern, Switzerland.

[c] Pathology Unit, Department of Molecular Biology and Translational Research, National Cancer Institute and Center for Molecular Biomedicine, Aviano (PN), Italy.

[d] Doctoral School in Molecular Biomedicine, University of Trieste, 34100 Trieste, Italy.

[e] Department of Chemistry, University of Illinois at Urbana-Champaign, 600 S. Mathews Avenue, Urbana, IL 61801, USA.

[f] Department of Molecular Sciences and Nanosystems, Ca' Foscari University, Venezia 30123, Italy.

* Corresponding author.

E-mail address: carlotta.granchi@unipi.it (C. Granchi).

Keywords: Monoacylglycerol lipase inhibitors, MAGL, cancer, ketoxime.

Highlights

- 35 salicylketoxime derivatives were synthesized.

- Compounds **13a** and **14a** are potent reversible MAGL inhibitors.
- Compounds **13a** and **14a** proved to be selective for MAGL.
- Compounds **13a** and **14a** reduced the proliferation of a series of cancer cell lines.

ABSTRACT

Monoacylglycerol lipase (MAGL) is the enzyme hydrolyzing the endocannabinoid 2-arachidonoylglycerol (2-AG) to free arachidonic acid and glycerol. Therefore, MAGL is implicated in many physiological processes involving the regulation of the endocannabinoid system and eicosanoid network. MAGL inhibition represents a potential therapeutic target for many diseases, including cancer. Nowadays, most MAGL inhibitors inhibit this enzyme by an irreversible mechanism of action, potentially leading to unwanted side effects from chronic treatment. Herein, we report the discovery of long-chain salicylketoxime derivatives as potent and reversible MAGL inhibitors. The compounds herein described are characterized by a good target selectivity for MAGL and by antiproliferative activities against a series of cancer cell lines. Finally, modeling studies suggest a reasonable hypothetical binding mode for this class of compounds.

1. Introduction

Monoacylglycerol lipase (MAGL) is a 33 kDa serine hydrolase that peripherally (i.e. adipose tissue, liver, etc.) cleaves monoacyglycerols to fatty acids and glycerol. In particular, in the central nervous system, MAGL is the main enzyme responsible of the degradation of 2-arachidonoylglycerol (2-AG) to arachidonic acid and glycerol. 2-AG is one of the two major endocannabinoids, the other being anandamide (AEA), which is instead hydrolyzed by the enzyme fatty acid amide hydrolase (FAAH) [1]. 2-AG is produced on demand and represents one of the most important endogenous ligands that activate the G protein-coupled cannabinoid receptors, CB1 and CB2. Therefore, 2-AG is involved in

the modulation of many pathological and physiological processes, including pain, inflammation, appetite, memory and emotion.

In 2011, a functional proteomic analysis of a panel of aggressive and non-aggressive human cancer cell lines from multiple tumors was conducted in order to identify enzyme activities that contributed to cancer pathogenesis, and it was found that MAGL levels were consistently more elevated in aggressive cancer cells than in their non-aggressive counterparts. Moreover, it was demonstrated that MAGL was responsible for high serine hydrolase activities found in aggressive cancer cells [2–4]. It is intriguing that the mechanism of cancer aggressiveness provoked by elevated MAGL activity involves the supply of fatty acids for the production of pro-tumorigenic signaling lipids: MAGL controls the pools of free fatty acids that are the building blocks for these pro-tumorigenic signaling lipids, such as prostaglandin E2 (PGE2) and lysophosphatidic acid (LPA) [5]. MAGL blockade leads to an accumulation of the endocannabinoid 2-AG, thus suppressing arachidonic acid formation and the consequent production of pro-inflammatory prostaglandins [6]. At the same time the inhibition of the enzymatic degradation of 2-AG leads to amplified effects on CB1, indirectly enhancing endocannabinoid signaling without causing the problems that are typical of CB1 agonists [5,7,8]. Therefore, inhibition of MAGL was found to reduce pain, inflammation, anxiety, nausea and depression. Considering these multiple beneficial effects, from a therapeutic point of view, it is clear that MAGL is a promising target for cancer as well as for other pathologies, such as chronic pain or inflammatory diseases.

Most of the MAGL inhibitors so far reported in the literature bind irreversibly to the enzyme. However, chronic and irreversible MAGL inactivation is often associated with CB1 receptor desensitization leading to unwanted effects, such as functional antagonism at CB1 receptors and physical dependence [9]. Presently, only few of the currently discovered MAGL inhibitors show a reversible mode of action, although this mode of action is considered to be a preferable and potentially safer alternative to irreversible inhibition [10]. Two widely known examples of irreversible and potent inhibitors are JZL184 (4-nitrophenyl-4-[bis(1,3-benzodioxol-5-yl)(hydroxy)methyl]piperidine-1-

carboxylate **1**, Figure 1)[11] and CAY10499 (benzyl(4-(5-methoxy-2-oxo-1,3,4-oxadiazol-3(2H)-yl)-2-methylphenyl)carbamate **2**, Figure 1) [12]. To the best of our knowledge, the naturally occurring terpenoids Euphol (**3**, Figure 1) and Pristimerin (**4**, Figure 1) are the first reversible MAGL inhibitors ever reported. However, these two compounds act on a large number of secondary targets; therefore, they are unsuitable for further development as MAGL inhibitors [13,14]. Another MAGL inhibitor from natural sources is the triterpenoid β-amyrin, structurally related to Pristimerin and Euphol, although it was found to be more active on other hydrolases than on MAGL [7].

Hernández-Torres *et al.* reported a MAGL inhibitor c21 (benzo[d][1,3]dioxol-5-ylmethyl 6-([1,1′-biphenyl]-4-yl)-hexanoate **5**, Figure 1), which was demonstrated to improve the clinical outcome of multiple sclerosis *in vivo* using the experimental allergic encephalomyelitis mouse model and for the first time it was observed that the therapeutic effects of this reversible inhibitor were not accompanied by catalepsy or other motor impairments that often occur after the administration of irreversible inhibitors [15]. More recently, a growing number of reversible MAGL inhibitors have been reported, such as (4-(4-chlorobenzoyl)piperidin-1-yl)(3-hydroxyphenyl)methanone **6** (Figure 1), a nanomolar inhibitor developed by our group, which originated from an optimization study of an initial compound discovered by a virtual screening procedure [16,17] and (4-benzylpiperidin-1-yl)(5-(4-hydroxyphenyl)-1-(3-methylbenzyl)-1H-pyrazol-3-yl)methanone **7** (Figure 1), which was found to relieve the neuropathic hypersensitivity induced *in vivo* by oxaliplatin [18]. A loratidine analogue was recently discovered as a potent MAGL inhibitor that also showed anti-histaminergic activity, making it a potentially useful agent in inflammatory pathologies in which the simultaneous blockade of these targets would be desirable [19].

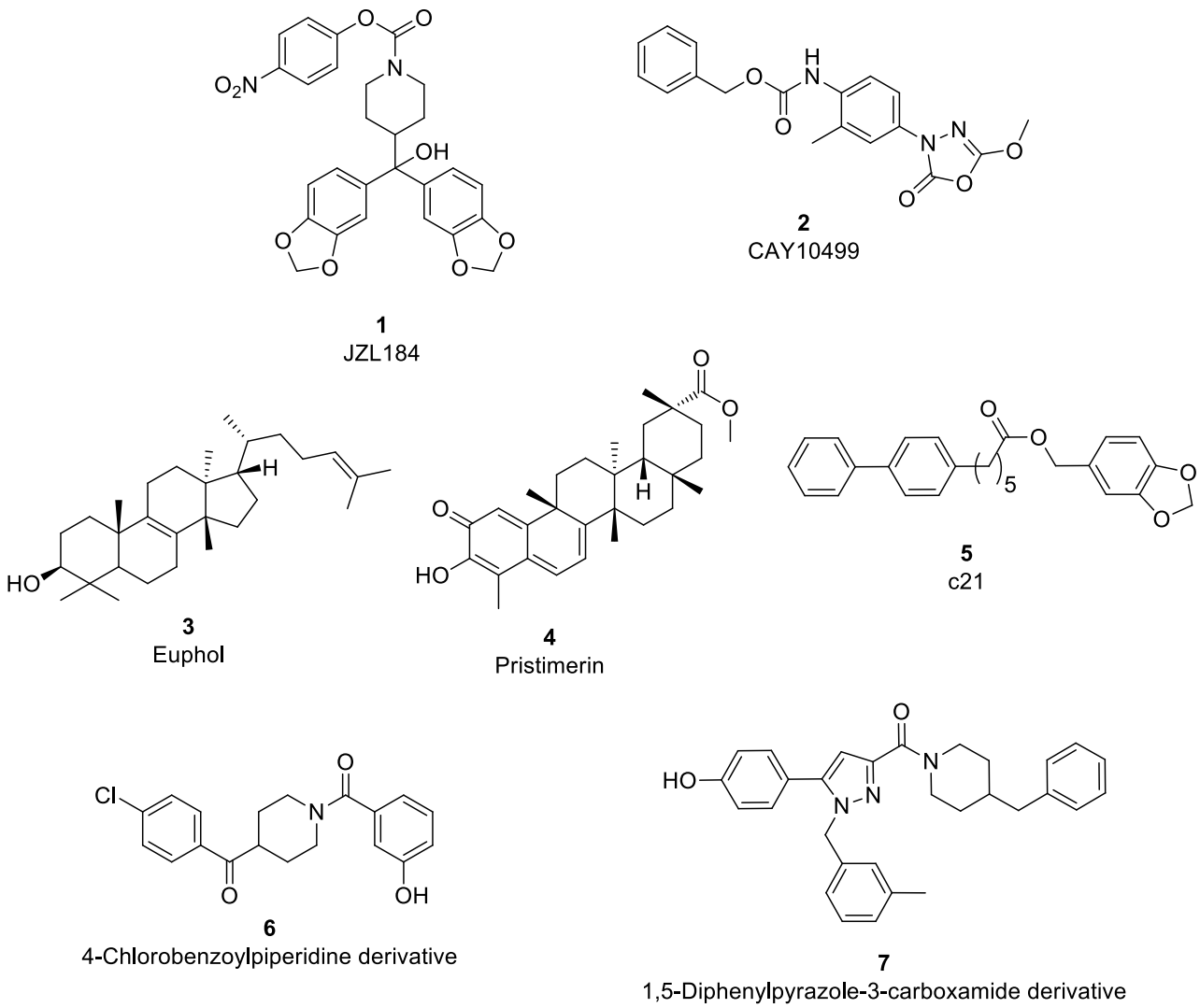

Figure 1. Structures of some of the most relevant MAGL inhibitors.

In the search for new MAGL inhibitors, we screened an in-house library of published compounds, and we found that compounds **8** and **9** (Figure 2) showed a certain inhibition of MAGL activity, with IC_{50} values of 34 and 11 µM, respectively. These two compounds, which were previously developed as estrogen receptor ligands [20], share the same salicylketoxime scaffold, with a peripheral phenolic ring substituted with a fluorine atom in a position *ortho* to the hydroxyl group, and differ only in the alkyl group of the ketoxime moiety. In particular, we observed about a three-fold increase of activity in passing from the methyl (compound **8**) to the ethyl ketoxime substituent (compound **9**), thus suggesting a possible improvement in inhibitory activity by further increasing the length of this alkyl

chain. This trend is reasonable considering that the MAGL active site normally hosts the substrate 2-AG, which is a very long-chain ester of arachidonic acid and glycerol. Therefore, the presence of long alkyl chains or bulky groups are likely to be well tolerated by the enzyme, and the establishment of lipophilic interactions between molecules having long alkyl chains and the enzyme active site could enhance the inhibitory potency of such compounds.

These data prompted us to further develop this scaffold and generate new derivatives, by introducing the following modifications on the parent compounds **8** and **9**: *a*) we progressively increased the length of the linear saturated ketoximic alkyl chain in compounds **10-15**. In fact, compounds **10a-d** have relatively small chains with 4 carbon atoms (n = 3, Figure 2), while compounds **11a-d**, **12a-d**, **13a-d**, **14a-d** and **15a-d** have gradually longer groups with 7, 9, 11, 13 or 15 carbon atoms, respectively (n = 6, 8, 10, 12, 14, Figure 2); *b*) simple aromatic groups in the ketoxime moiety were also explored, in particular a phenyl ring (n = 0, compounds **16a-d**, Figure 2) or a benzyl group (n = 1, compounds **17a-d**, Figure 2); *c*) in all the previous compounds mentioned at points *a*) and *b*), we varied the substituents of the peripheral phenolic ring, in order to determine their importance; therefore, we initially maintained the *p*-OH/*m*-F substitution pattern (R_2 = OH, R_1 = F, compounds "**a**" of Figure 2), and we also introduced the relative methoxylated derivatives (R_2 = OCH_3, R_1 = F, compounds "**b**" of Figure 2). Moreover, we removed the fluorine atom to assess its role in the inhibitory activity of these compounds, thereby obtaining the *p*-hydroxyl derivatives (R_2 = OH, R_1 = H, compounds "**c**" of Figure 2) and the related *p*-methoxy analogues (R_2 = OCH_3, R_1 = H, compounds "**d**" of Figure 2). Finally, in order to acquire information about the binding mode of this class of compounds, the last modifications were applied only to compound **14**, which had shown the best enzymatic inhibitory activity: we either removed all the substituents on the peripheral phenyl ring, or introduced a fluorine atom or a hydroxyl group in the *meta* position (compounds **14e-g**, Figure 2).

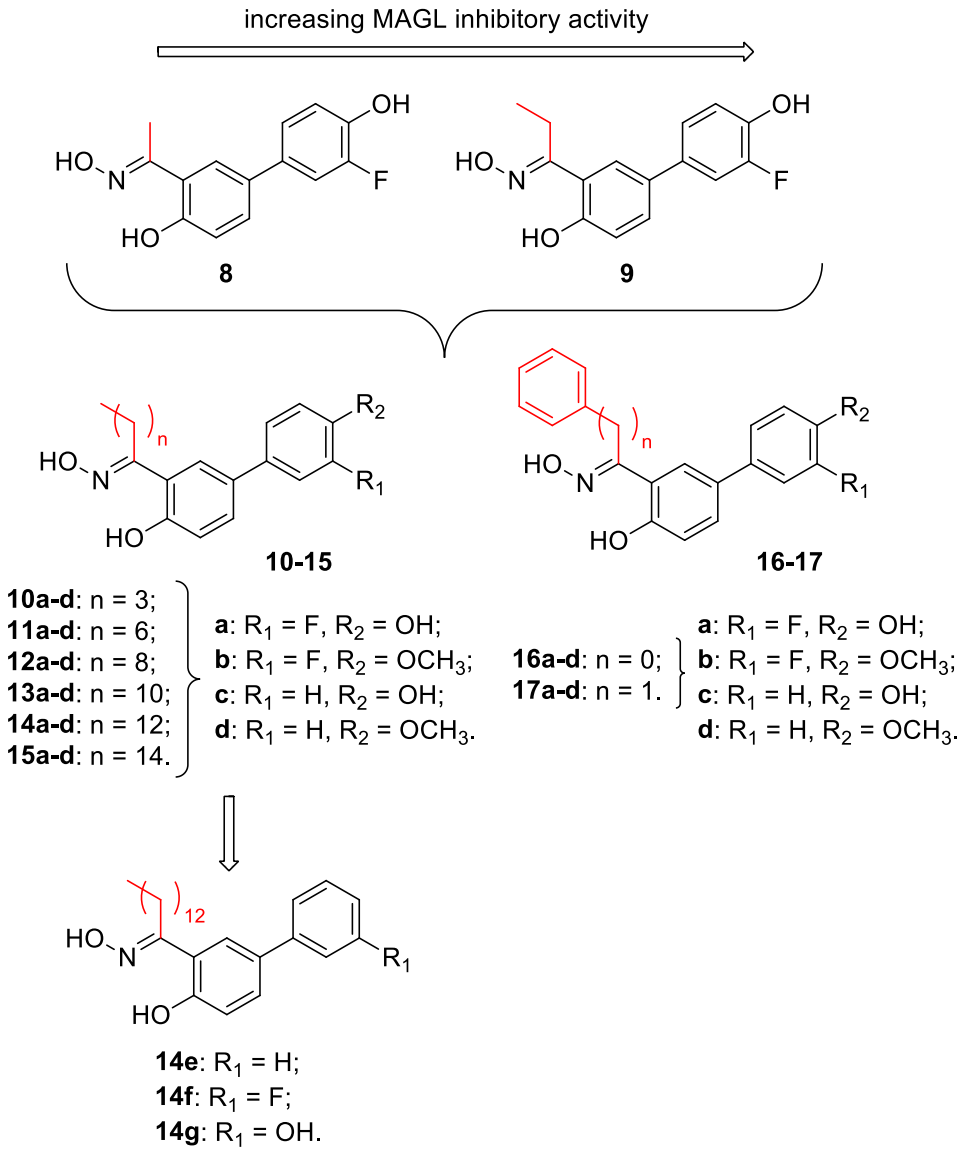

Figure 2. Design of salicylketoximes with bulky chains (in red): starting compounds **8** and **9** and newly designed derivatives, bearing alkyl (**10-15**) or aromatic chains (**16-17**).

2. Results and discussion

2.1. Chemistry

The synthesis of derivatives **10-15** started from the corresponding commercially available carboxylic acid, valeric acid **18** (n = 3, Scheme 1), ottanoic acid **19** (n = 6, Scheme 1), decanoic acid **20** (n = 8, Scheme 1), dodecanoic acid **21** (n = 10, Scheme 1), mirystic acid **22** (n = 12, Scheme 1) or palmitic

acid **23** (n = 14, Scheme 1), which was converted to the acid chloride by refluxing it with thionyl chloride for three hours. After evaporation of the excess of $SOCl_2$, the acid chloride was subjected to a Friedel-Crafts reaction with 4-bromoanisole in the presence of aluminum trichloride and 1,2-dichloroethane as the solvent: as expected, the acylation was directed to the *meta* position with respect to the bromine atom, but at the same time we also observed the desired demethylation of the methoxy group, thus giving derivatives **24-29** directly (Scheme 1). The acylated intermediates were subjected to a Pd-catalyzed cross-coupling reaction under classical Suzuki conditions [21], with the appropriate arylboronic acid: 3-fluoro-4-methoxyphenylboronic acid for intermediates **30**, **32**, **34**, **36**, **38** and **40**, 4-methoxyphenylboronic acid for compounds **31**, **33**, **35**, **37**, **39** and **41**, phenylboronic acid for compound **42**, 3-fluorophenylboronic acid for compound **43** and 3-methoxyphenylboronic acid for compound **44** (Scheme 1). The biaryl derivatives obtained were in part *O*-demethylated with BBr_3 at 0 °C to afford free phenols **45-57**. All the resulting phenolic derivatives **45-57**, their methoxylated precursors **30-41** and compounds **42** and **43**, bearing no substituents or only a *m*-fluorine group, respectively, were directly transformed into the corresponding salicylketoximes **10a-d**, **11a-d**, **12a-d**, **13a-d**, **14a-g** and **15a-d** by a condensation reaction with hydroxylamine hydrochloride in ethanol (Scheme 1).

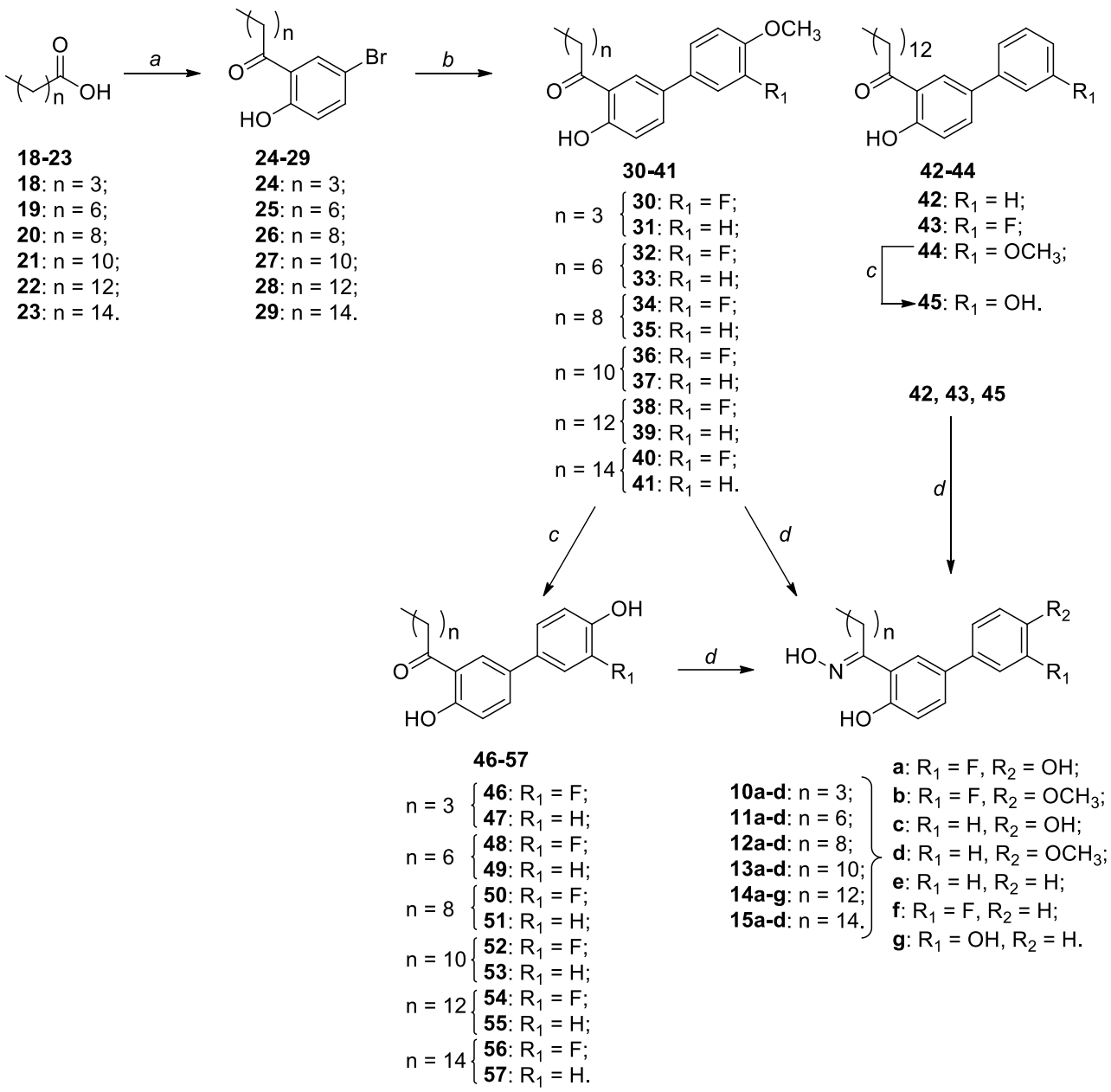

Scheme 1. Synthesis of salicylketoximes **10-15**. Reagents and conditions: a) i. $SOCl_2$, 95 °C, 3 h; ii. 4-bromoanisole, $AlCl_3$, DCE, 65 °C, 2 h; b) $ArB(OH)_2$, $Pd(OAc)_2$, PPh_3, aqueous 2 M Na_2CO_3, toluene/EtOH (1:1), 100 °C, 24 h; c) BBr_3, CH_2Cl_2, - 10 °C to 0 °C, 1 h; d) $NH_2OH{\cdot}HCl$, EtOH, 50 °C, 12-48 h.

Salicylketoximes **16-17**, bearing an aromatic substituent such as phenyl (n = 0, Scheme 2) or benzyl (n = 1, Scheme 2) in the ketoximic portion, were prepared following a similar synthetic scheme,

differing only for the initial step in which the starting acid chlorides were commercially available (benzoyl chloride **58** or phenylacetyl chloride **59**) and were directly used in the Friedel-Crafts reaction (step *a*, Scheme 2). Both the methoxylated derivatives **62-65** as well as the phenolic intermediates **66-69** were transformed in the corresponding oxime derivatives **16a-d** and **17a-d** by a condensation reaction with hydroxylamine hydrochloride in ethanol under mild heating.

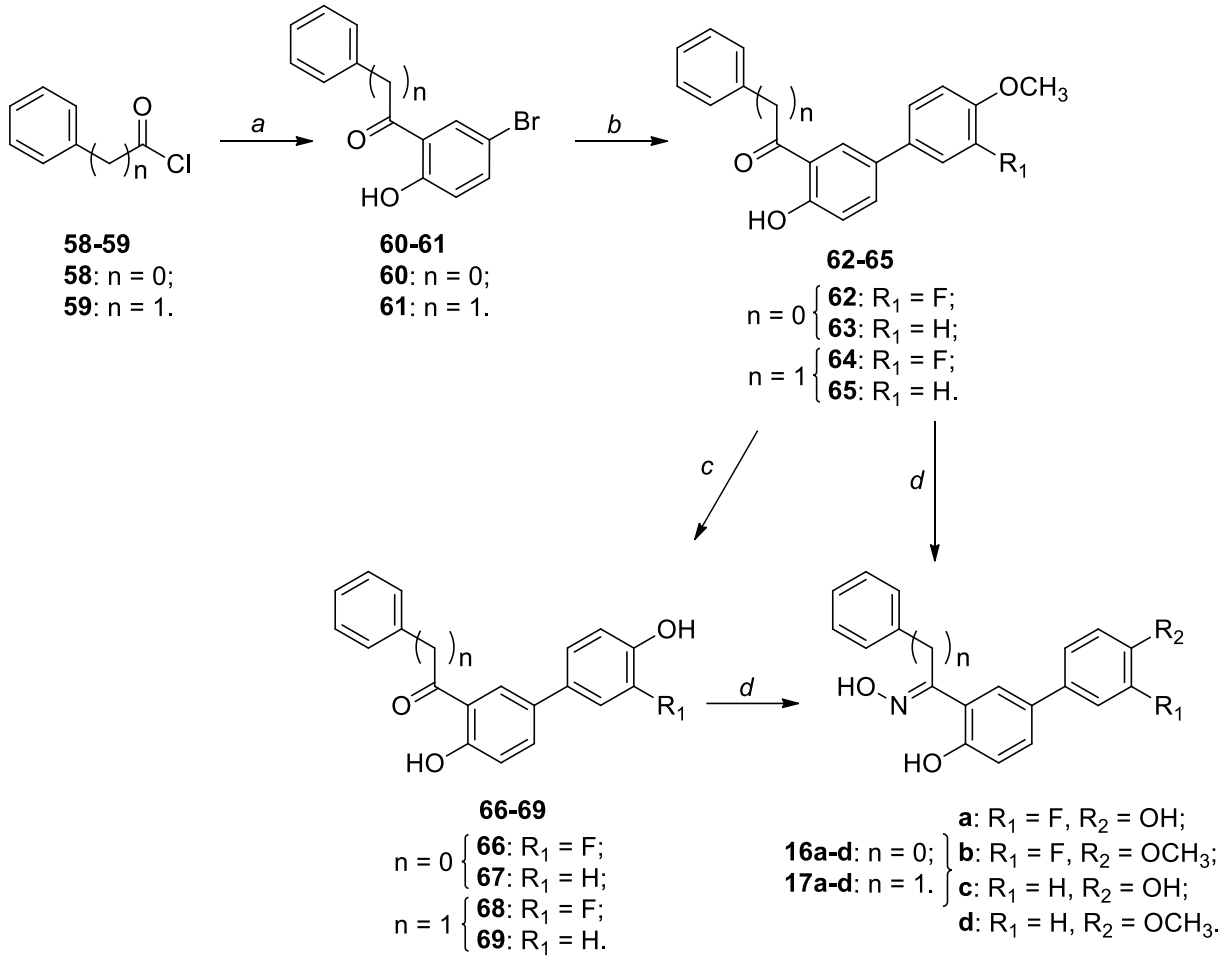

Scheme 2. Synthesis of salicylketoximes **16-17**. Reagents and conditions: a) 4-bromoanisole, $AlCl_3$, DCE, 65 °C, 2 h; b) $ArB(OH)_2$, $Pd(OAc)_2$, PPh_3, aqueous 2 M Na_2CO_3, toluene/EtOH (1:1), 100 °C, 24 h; c) BBr_3, CH_2Cl_2, - 10 °C to 0 °C, 1 h; d) $NH_2OH{\cdot}HCl$, EtOH, 50 °C, 12-48 h.

Finally, we decided to insert an isopropyl group as the ketoximic chain, in order to compare the biological results obtained from compounds **10a-d**, **11a-d**, **12a-d**, **13a-d**, **14a-g** bearing long linear

alkyl chains with those of compounds **16a-d** and **17a-d** possessing bulky aromatic groups. The isopropyl-substituted compounds **76** and **77** (Scheme 3) may represent an intermediate situation between very flexible chains and highly bulky groups. These two compounds differ only for the presence of an additional fluorine atom in *meta* position of the peripheral phenolic ring of compound **76**, which is not present in compound **77**, since in other analogues of this series these two substitution combinations gave the best results in enzymatic assays (see section 2.2. MAGL enzymatic assays). Compounds **76** and **77** were prepared following the same synthetic scheme described above starting from isobutyryl chloride **70**, which was subjected to a Friedel-Crafts reaction to produce phenol **71**. A cross-coupling reaction with the properly substituted phenylboronic acid gave compounds **72** and **73**. These biphenylic compounds were subjected to a BBr_3-promoted demethylation of the methoxy group and the resulting compounds **74** and **75** were then reacted with hydroxylamine hydrochloride to obtain the final ketoximic products.

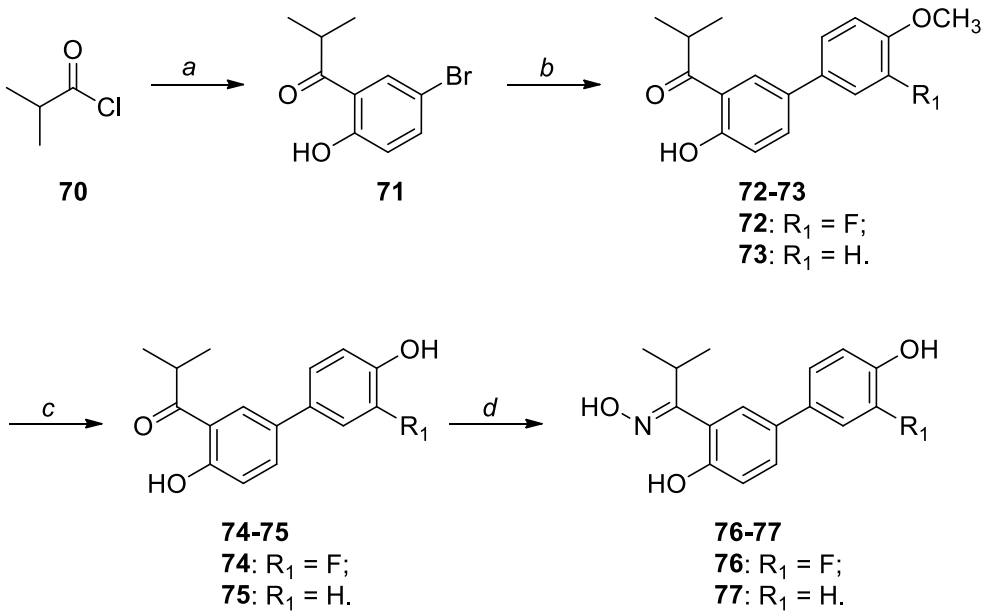

Scheme 3. Synthesis of salicylketoximes **76-77**. Reagents and conditions: a) 4-bromoanisole, $AlCl_3$, DCE, 65 °C, 2 h; b) $ArB(OH)_2$, $Pd(OAc)_2$, PPh_3, aqueous 2 M Na_2CO_3, toluene/EtOH (1:1), 100 °C, 24 h; c) BBr_3, CH_2Cl_2, - 10 °C to 0 °C, 1 h; d) $NH_2OH{\cdot}HCl$, EtOH, 50 °C, 24-72 h.

2.2. MAGL enzymatic assays

The synthesized compounds were tested for their inhibitory activity on human MAGL (Table 1) together with the known irreversible MAGL inhibitor CAY10499 (**2**) and the (4-(4-chlorobenzoyl)piperidin-1-yl)(3-hydroxyphenyl)methanone **6**, which were used as reference compounds. Moreover, the new compounds were compared with the parent methylketoxime **8** and ethylketoxime **9**.

We observed a common trend in the *p*-OH, *m*-F-phenyl- and *p*-OH-phenyl-substituted series of compounds bearing alkyl chains: the potency of inhibition increases in parallel with the number of methylene units in the alkyl ketoximic chain; therefore, as long as the length of this chain increases, the compounds become more potent, eventually reaching nanomolar inhibition values. In particular, this trend was observed when n = 10, 12 or 14 in the *p*-OH *m*-F group (compounds **13a**, **14a** and **15a**), and when n = 12 or 14 (compounds **14c** and **15c**) for the *p*-OH group. We were pleased to observe these encouraging results from these newly developed compounds, because it confirmed our initial hypothesis regarding the correlation between chain length and inhibitory activity. Indeed, the parental short-chain ketoximic derivatives **8** and **9** were about 50 or 16-fold less potent, respectively, than the best compound of this new series (**14a**).

Our data suggest that a further increase of the chain length over 12 carbons becomes detrimental for the interaction with the enzyme. The palmitoyl derivative (n = 14) showed a slight decrease of potency as compared to the myristoyl derivative (n = 12). In fact, compound **14a** resulted to be the most potent MAGL inhibitor of this series of compounds, showing an IC_{50} value of 0.68 µM. Compound **14a** is slightly more potent than the close analogue **13a** which bears a shorter chain (IC_{50} = 0.71 µM), and more active than compound **15a** (IC_{50} = 0.91 µM), which differs from **14a** only for an extra two methylene units. Similarly, the same behaviour was observed for the non-fluorinated *p*-OH substituted derivatives, among which **14c** was the most potent inhibitor (IC_{50} = 0.77 µM). When the

length of the alkyl chain was increased over 12 carbons, there was a loss of potency (n = 14, compound **15c**, IC_{50} = 0.96 μM).

From the comparison between the just-mentioned series of derivatives, it is reasonable to state that the presence of the fluorine atom in combination with the hydroxyl group led to a slight improvement of activity with respect to the analogue phenolic compound without the fluorine atom (i.e., comparison between **14a** and **14c**). This fact could be explained by considering that the electron-withdrawing fluorine atom increases the acidity of the adjacent OH group, increasing its polarization, and thus enhancing its ability to establish hydrogen bonds (see Molecular modeling section). Poorer activities were generally obtained with the compounds possessing aromatic ketoximic chains: both the benzyl and phenyl-substituted compounds showed similar activities in the low micromolar range, and also in this case the fluorine-bearing compounds **16a** and **17a** (IC_{50} = 1.7 μM for both of them) proved to inhibit MAGL with a higher potency compared to compounds **16c** and **17c** (IC_{50} value of 7.2 and 4.8 μM, respectively).

Overall these data suggest that the presence of a long aliphatic chain in the ketoxime moiety is well tolerated by the enzyme, but bulkier and less flexible groups, such as a phenyl or a benzyl ring, lead to a detrimental loss of activity. However, the length of the alkyl chain reaches a sort of "plateau" at n = 12, after which a further increase results in a significant decrease of the biological activity. In order to confirm the importance of the *p*-hydroxy group, the relative methoxylated derivatives were tested (series "**b**" and "**d**"): all these compounds were less active than their hydroxylated counterparts, with IC_{50} values in the range of 12-119 μM or greater than 200 μM.

Since compound **14a** was the most promising compound of this class of derivatives, with an inhibitory potency that was even higher than that of reference compound **6**, we decided to further explore substitutions on the peripheral phenyl ring. Removal of all the substituents (**14e**) or the presence of a *meta*-fluoro or a *meta*-hydroxy group (**14f** and **14g**, respectively) resulted in only modest inhibition of enzyme activity for all the three compounds; the 3 to 37-fold decrease of activity for these

derivatives supported the hypothesis that the *p*-hydroxy *m*-fluoro substitution pattern is a key to improve inhibition of MAGL activity.

For what concerns *i*-propyl-substituted compounds **76** and **77**, they showed IC_{50} values in the low micromolar range (IC_{50} = 3.3 µM for **76** and 5.1 µM for **77**). Compound **76** was slightly less active than the other corresponding *p*-OH/*m*-F substituted compounds, such as the bulkier aryl derivatives **16a** and **17a** (IC_{50} = 1.7 µM), or the compounds bearing linear alkyl chains **10a-15a** (IC_{50} = 0.68-2 µM). Compound **77** showed approximately the same inhibition potency as those displayed by *p*-OH substituted compounds **16c** and **17c** (IC_{50} = 4.8-7.2 µM) and by compound **10c** bearing the shortest linear chain (IC_{50} = 5.2 µM), whereas its activity was lower than those of compounds **11c-15c** with longer alkyl chains (IC_{50} = 0.77-2.5 µM). These two *i*-propyl-substituted compounds maintain the same trend that was observed for the previous series of compounds, which consisted in an inhibition activity improvement given by the additional presence of the fluorine atom in *ortho* position to the phenolic hydroxyl group.

Table 1. MAGL inhibitory activity of compounds **2**, **6**, **8**, **9 10a-d**, **11a-d**, **12a-d**, **13a-d**, **14a-g**, **15a-d**, **16a-d**, **17a-d**, **76** and **77**.

Compound	Structure	IC_{50} (mean ± SD, µM)
CAY10499 (**2**)	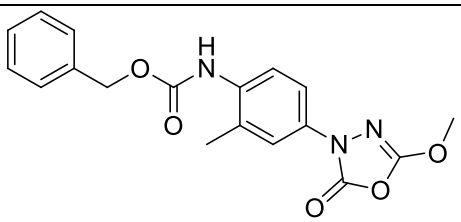	0.14 ± 0.03
6	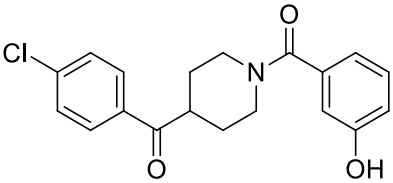	0.84 ± 0.04
8	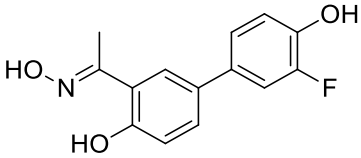	34 ± 1

9	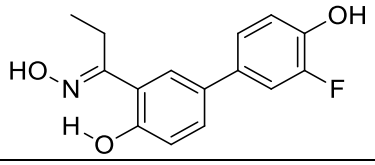		11 ± 2
10a	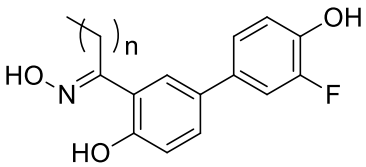	n = 3	2.0 ± 0.1
11a		n = 6	1.3 ± 0.2
12a		n = 8	1.0 ± 0.2
13a		n = 10	0.71 ± 0.03
14a		n = 12	0.68 ± 0.01
15a		n = 14	0.91 ± 0.02
16a	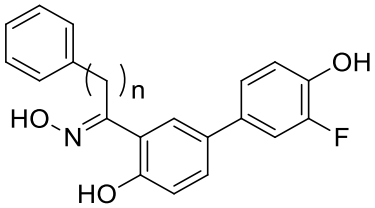	n = 0	1.7 ± 0.9
17a		n = 1	1.7 ± 0.1
10b	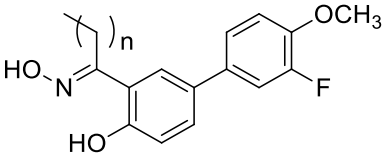	n = 3	36 ± 2
11b		n = 6	16 ± 1
12b		n = 8	19 ± 3
13b		n = 10	53 ± 3
14b		n = 12	> 200
15b		n = 14	>200
16b	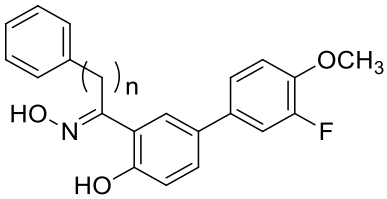	n = 0	26 ± 5
17b		n = 1	12 ± 1
10c	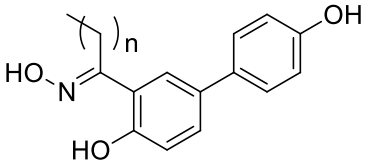	n = 3	5.2 ± 0.2
11c		n = 6	2.5 ± 0.2
12c		n = 8	1.5 ± 0.3
13c		n = 10	1.1 ± 0.1
14c		n = 12	0.77 ± 0.04
15c		n = 14	0.96 ± 0.14
16c	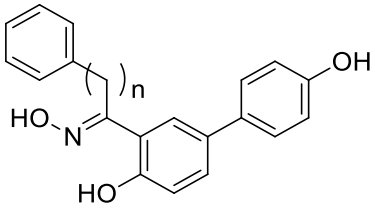	n = 0	7.2 ± 0.4
17c		n = 1	4.8 ± 0.2
10d		n = 3	119 ± 13
11d		n = 6	30 ± 2
12d		n = 8	36 ± 4

13d	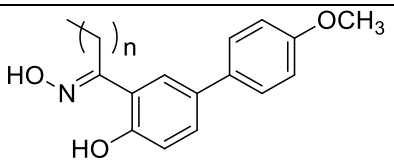	n = 10	69 ± 6
14d		n = 12	28 ± 3
15d		n = 14	70 ± 5
16d	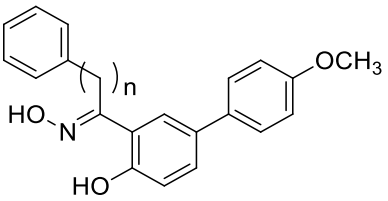	n = 0	34 ± 3
17d		n = 1	20 ± 1
14e	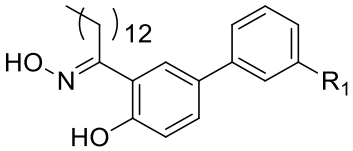	R_1 = H	25 ± 5
14f		R_1 = F	18 ± 3
14g		R_1 = OH	2.4 ± 0.5
76	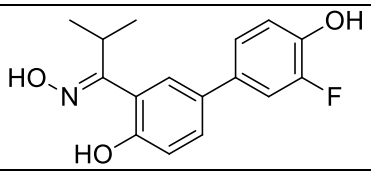	R_1 = F	3.3 ± 0.5
77		R_1 = H	5.1 ± 0.4

In order to verify whether the compounds could interact with the cysteines of the MAGL enzyme, the activity of the most potent inhibitor **14a** was also tested in the presence of the thiol-containing agent 1,4-dithio-DL-threitol (DTT). It is known that MAGL is sensitive to inhibition by sulfhydryl-specific agents, since some compounds reported in literature irreversibly inhibit MAGL, being involved in a Michael addition reaction that leads to covalent modifications of some key cysteine residues, such as Cys201, Cys208 or Cys242 [22–24]. DTT-based experiments were used as a first demonstration that these compounds are reversible MAGL inhibitors, ruling out their covalent interactions with cysteines. As shown in Figure 3A, the IC_{50} value of compound **14a** was only very slightly, but not significantly, influenced by the presence of DTT, shifting from 0.68 µM when assayed in the absence of DTT to 0.70 µM when assayed in the presence of 10 µM DTT, thus excluding any interaction of these compounds with the cysteine residues present in MAGL. Furthermore, with the aim of establishing whether the mechanism of inhibition was reversible or irreversible, the effects of dilution and preincubation on the inhibitory activity of compound **14a** were evaluated. In case of an irreversible inhibition, potency should not decrease after dilution, whereas in case of a reversible inhibition, the potency level should be substantially reduced after dilution [24]. In our experiment,

the inhibition produced by preincubation with a 20 µM concentration of **14a** was measured after a 40X dilution and compared to the potency observed by a 20 µM and a 0.5 µM of compound **14a**. As shown in Figure 3B, the results were consistent with a reversible inhibition mechanism, as the inhibition produced by 0.5 µM of the compound was similar to that after a 40X dilution and was different to that produced by the compound at a concentration of 20 µM. As a second test of mechanism, the biological activity of **14a** was also tested at different preincubation times of compound with MAGL. In this assay, the compound was preincubated with the enzyme for 0, 30 and 60 minutes before adding the substrate to start the enzymatic reaction. An irreversible inhibitor should show a higher potency after longer incubation times, whereas a reversible inhibitor should show a constant inhibition potency that was independent of the incubation time. As shown in Figure 3C, this assay confirmed the reversible property of **14a**, as it did not show any significant increase in inhibitory potency at longer incubation times.

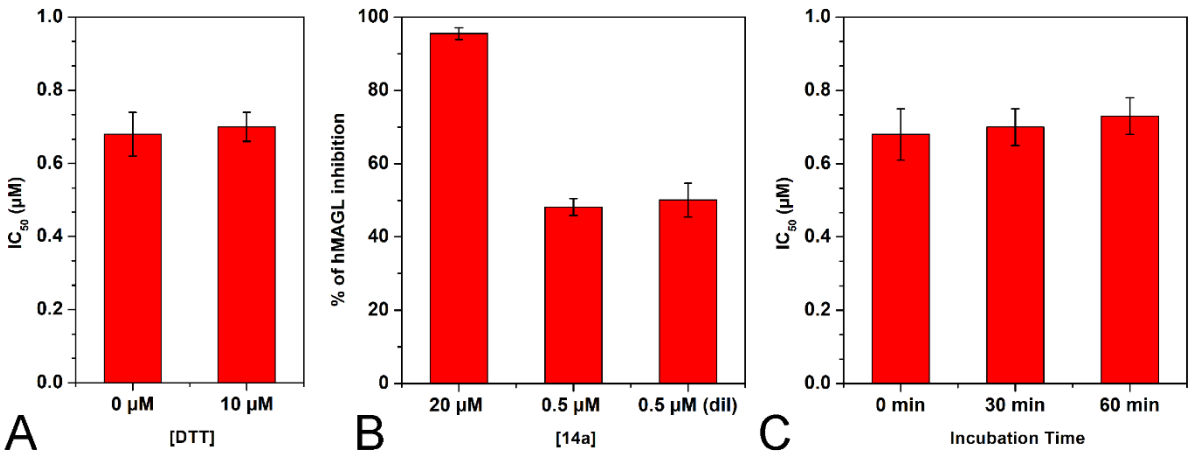

Figure 3. Compound **14a**-MAGL inhibition analysis. A) Effect of DTT on the MAGL inhibition properties. B) Dilution assay: the first two columns indicate the inhibition percentage of compound **14a** at a concentration of 20 µM and 0.5 µM. The third column indicates the inhibition percentage of compound **14a** after dilution (final concentration = 0.5 µM). C) IC_{50} (µM) values of **14a** at different preincubation times with MAGL (0 min, 30 min and 60 min).

2.3. Selectivity towards other targets

With the aim of evaluating the selectivity of the most potent MAGL inhibitors towards the other targets of the endocannabinoid system, compounds **13a** and **14a** were tested on FAAH, ABHD6, ABHD12 and cannabinoid receptors CB1 (CB1R) and CB2 (CB2R) (Table 2). Both compounds had low activity on ABHD6 and ABHD12 (IC_{50} values greater than 10 µM), and only a weak activity on FAAH (IC_{50} = 4.1 and 8.7 µM for **13a** and **14a**, respectively). The binding data showed that compounds **13a** and **14a** have a moderate affinity towards CB1R (K_i values of 2.6 and 4.1 µM for **13a** and **14a**, respectively), while they do not bind to CB2R at the concentration of 10 µM (5% of binding, data not shown). The long alkyl chain present in the structure of the salicylketoxime derivatives **13a** and **14a** resembles the arachidonoyl tail of the endocannabinoids AEA and 2-AG, and this may be responsible of the moderate effects observed on FAAH and CB1R. However, as AEA and 2-AG have different affinities for CB1R and CB2R and the degrading enzymes, our compounds **13a** and **14a** also showed a preferential binding towards MAGL as compared to FAAH (selectivity factor = 6 and 13 for **13a** and **14a**, respectively), ABHDs (selectivity factor ≥ 14 for **13a** and **14a**), CB1R (selectivity factor = 4 and 6 for **13a** and **14a**, respectively) and CB2R (selectivity factor ≥ 15 for **13a** and **14a**).

Table 2. Biological activities (IC_{50} values for FAAH, ABHD6 and ABHD12 and K_i values for CB1R and CB2R, means ± SD) of compounds **13a** and **14a** on the major components of the endocannabinoid system.

	IC_{50} (mean ± SD, µM)			**K_i (mean ± SD, µM)**	
Compound	**FAAH**	**ABHD6**	**ABHD12**	**CB1R**	**CB2R**
13a	4.1 ± 1.3	> 10	> 10	2.6 ± 0.8	> 10
14a	8.7 ± 1.8	> 10	> 10	4.1 ± 1.1	> 10

Considering that the scaffold of these molecules derives from a structural evolution that started from compounds previously developed as estrogen receptor ligands [20], we decided to test whether the newly synthesized compounds maintained a certain affinity for ERα and ERβ. The binding affinity for ERα and ERβ of salicylketoximes **13a** and **14a**, showing the best inhibitory potency on MAGL, was measured by a radiometric competitive binding assay with [^{3}H]estradiol, using previously reported methods [25,26]. The relative binding affinity (RBA) values for the newly reported compounds are summarized in Table 3. RBA values are reported as percentage (%) of that of estradiol, which is set at 100% and compared to those of the initial compound **9**. Compound **9** showed very similar values to those previously published, which showed good affinity and selectivity for ERβ, compared to estradiol. Differently, both the new compounds, **13a** and **14a**, had a negligible affinity for ERα and a very low residual affinity for ERβ, which appears to decrease with the increasing length of the ketoximic chain (Table 3). In fact, ethyl-substituted derivative **9** had a >5-fold greater ERβ affinity than that of compound **13a** (n = 10, Figure 2), which showed a RBA value of 6.8. The ERβ affinity of the longer-chain derivative **14a** (n = 12, Figure 2) was found to be further reduced (RBA = 2.6), being 2.6-fold lower than that of **13a**.

Table 3. Relative Binding Affinities of compounds **9**, **13a** and **14a** for the Estrogen Receptors α and β (RBA, %)[a]

Compound	**ERα**	**ERβ**
Estradiol	(100)	(100)
9	2.1	37
13a	0.31	6.8
14a	0.17	2.6

[a]This long-used binding assay has a coefficient of variation of 0.3.

2.4. Antiproliferative assays

Compounds **13a** and **14a** were also selected for further *in vitro* experiments to evaluate their antiproliferative potency against cancer cells. Compound CAY10499 (**2**) was used as the reference compound. Due to the key role that MAGL plays in the tumor progression of breast, colon and ovarian cancers [4,27,28], five tumor cell lines were chosen: the human breast MDA-MB-231, the colorectal HCT116 and the ovarian CAOV3, OVCAR3 and SKOV3 cancer cells (Table 4). Salicylketoximes **13a** and **14a** produced an appreciable inhibition of cell viability in all the tested cell lines, with IC_{50} values ranging from 7.6 to 73 µM. With respect to the covalent reference inhibitor CAY10499, both compounds **13a** and **14a** showed a more potent cytotoxic activity on CAOV3 and MDA-MB-231, with IC_{50} values of 11 and 7.6 µM for **13a**, respectively, and of 14 and 11 µM for **14a**, respectively (IC_{50} = 92 and 89 µM, respectively, for CAY10499). The proliferation of the HCT116 tumor cells was similarly affected by **13a** and CAY10499, whereas **14a** was slightly less potent (about 1.7-fold). Finally, compounds **13a** and **14a** exerted good antiproliferative potency on OVCAR3 and SKOV3, always maintaining better activities than those of the reference inhibitor (IC_{50} ranging from 20 to 40 µM for ketoxime derivatives *vs.* 34 and 50 µM of CAY10499).

Table 4. Cell growth inhibitory activities (IC_{50} values) of compounds **2**, **13a**, **14a**.

	IC_{50} (mean ± SD, µM)				
Compound	**HCT116**	**MDA-MB-231**	**CAOV3**	**OVCAR3**	**SKOV3**
CAY10499 (**2**)	42 ± 2	89 ± 4	92 ± 5	50 ± 3	34 ± 3
13a	45 ± 5	7.6 ± 1.2	11 ± 2	40 ± 6	20 ± 2
14a	73 ± 6	11 ± 1	14 ± 1	28 ± 2	26 ± 2

2.5. Molecular modeling

To suggest a possible binding mode for this class of derivatives, the interaction of compound **14a** with MAGL was analysed by means of docking and molecular dynamic (MD) simulations. This

compound was thus docked by using Autodock 4.2, and the best docking pose was subjected to 100 ns of MD simulation with explicit water molecules, as described in the Experimental section. Figure 4 shows the main interactions of **14a** with MAGL. The *p*-hydroxy-*m*-fluorophenyl fragment forms two H-bonds with the backbone nitrogen of A51 and the hydroxyl group of S122 in the oxyanion hole of the protein binding site. The biphenyl fragment shows lipophilic interactions with I179, V183, L184 and L241, whereas the salicylic hydroxyl group establishes an H-bond with the backbone nitrogen of D180 and forms a pseudocyclic system together with the oxime portion of the molecule. With regards to the alkyl chain, it occupies a portion of the binding site characterized by a high number of lipophilic residues and, in particular, it interacts with A151, A156, F159, L205, L213 and L214.

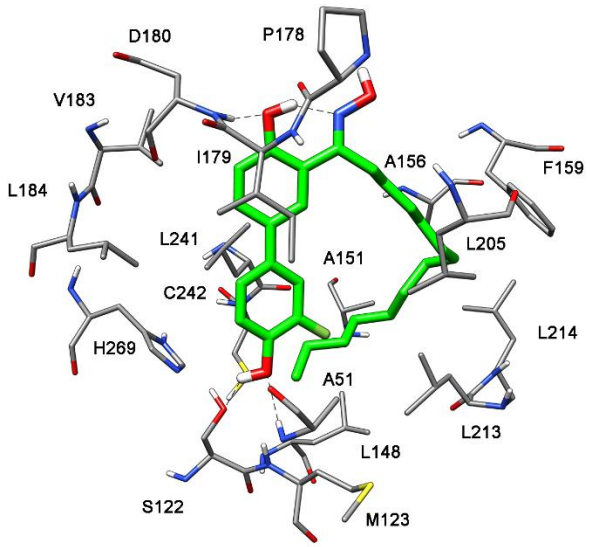

Figure 4. Minimized average structure of compound **14a** docked into MAGL.

2.6. Log*P* analysis

In order to have information about the lipophilic properties of the herein reported compounds, an evaluation of the log*P* has been carried out. Table 5 shows the consensus log*P* values obtained

through the Swiss ADME web tool [29], which combines five different log*P* calculation methods, and the clog*P* values calculated by DataWarrior software [30]. As shown in Figure S75, there is a good agreement between consensus and clog*P*, although this second method predicted log*P* values with a scaling factor of 1.24 ± 0.05 with respect to the consensus log*P*. As expected, the higher the number of carbon atoms in the compounds, the bigger the corresponding logP values calculated by both methods, with the maximum value obtained for compound **15b**. Nevertheless, no evident correlation between log*P* and activity of the different compounds was observed; in fact, by plotting the log*P* values against the measured pIC_{50} values of the ligands a correlation (R^2) lower than 0.1 was obtained (see Figure S76). Finally, from this analysis we can highlight that, comparing the two compounds **13a** and **14a** that showed the most promising activities, compound **13a** should be considered as the most promising candidate, since it shows a lower log*P* value than that of **14a**. It is worth mentioning that, although derivatives with moderate lipophilicity would be desirable to assure a good bioavailability and toxicity profile, ligands with a predominantly lipophilic nature could still be used for *in vivo* administration. As an example, compound **5** (Figure 1), for which a consensus log*P* value of 5.5 was predicted (Table 5), showed a suitable pharmacokinetic profile and demonstrated a pronounced activity in a mouse EAE *in vivo* model [15]. Nevertheless, structural optimization studies aimed at developing further salicylketoxime derivatives with improved ADME profiles and MAGL inhibition potencies will be performed in an attempt of developing better candidates for *in vivo* studies.

Table 5. Calculated consensus log*P* and clog*P* values for the reported compounds.

Compound	**Cons log*P***	**clog*P***
8	2.80	3.22
9	2.95	3.68
10a	3.68	4.58
11a	4.66	5.95
12a	5.53	6.86
13a	6.19	7.76

14a	6.91	8.67
15a	7.68	9.58
16a	3.84	4.48
17a	3.91	4.66
10b	4.05	4.86
11b	5.14	6.22
12b	5.90	7.13
13b	6.51	8.04
14b	7.30	8.95
15b	8.03	9.86
16b	3.13	3.50
17b	4.27	4.94
10c	3.48	4.48
11c	4.40	5.85
12c	5.22	6.76
13c	5.92	7.66
14c	6.60	8.57
15c	7.33	9.48
16c	3.50	4.38
17c	3.63	4.56
10d	3.78	4.76
11d	4.82	6.12
12d	5.59	7.03
13d	6.31	7.94
14d	7.00	8.85
15d	7.76	9.76
16d	3.92	4.65
17d	4.04	4.84
14e	7.02	8.92
14f	7.33	9.02
14g	6.61	8.57
76	3.40	3.89
77	3.07	3.79
5	5.50	6.58

3. Conclusions

In this work, we identified a series of long-chain salicylketoximes as MAGL inhibitors, starting from two compounds that had been previously designed as estrogen receptor ligands, and also showed an appreciable inhibition of MAGL activity. The newly developed compounds possess a long linear alkyl chain in the ketoxime moiety, thus gaining a low micromolar inhibition potency on MAGL and strongly reducing their affinity to ERα and ERβ. The most potent MAGL inhibitors herein reported

bear 12 or 14 carbon atom chains (compounds **13a** and **14a**) and molecular modeling studies confirmed that this chain is located in a lipophilic region of the enzyme active site. Nevertheless, in spite of their abundant lipophilic portion, these compounds also appear to establish hydrogen bonds with key residues of the protein. An enzymatic study of their binding mode revealed that these compounds are not cysteine binders, and they inhibit the enzyme reversibly. Moreover, the salicylketoximes had only moderate effects on the rest of the endocannabinoid system, since compound **14a** shows a MAGL-selectivity *vs.* FAAH, ABHDs and CBRs always greater that six-fold. Finally, these compounds were evaluated for their ability to reduce the proliferation of cancer cells, and they were particularly effective in both ovarian and breast cancer cell lines, thus supporting their potential role as anticancer agents.

4. Experimental section

4.1. Chemistry

All solvents and chemicals were purchased from Sigma-Aldrich and Alfa Aesar and used without further purification. Chromatographic separations were performed on silica gel columns by flash chromatography (Kieselgel 40, 0.040−0.063 mm; Merck). Reactions were followed by thin layer chromatography (TLC) on Merck aluminum silica gel (60 F254) sheets that were visualized under a UV lamp. Evaporation was performed in vacuo (rotating evaporator). Sodium sulfate was always used as the drying agent. Proton (^{1}H) and carbon (^{13}C) NMR spectra were obtained with a Bruker Avance III 400 MHz spectrometer (400 MHz for ^{1}H NMR and 100 MHz for ^{13}C NMR) using the indicated deuterated solvents. Chemical shifts are given in parts per million (ppm) (δ relative to residual solvent peak for ^{1}H and ^{13}C). ^{1}H NMR spectra are reported in this order: multiplicity and number of protons. Standard abbreviation indicating the multiplicity were used as follows: s = singlet, d = doublet, dd = doublet of doublets, ddd = doublet of doublet of doublets, dddd = doublet of doublet of doublet of doublets, t = triplet, tt = triplet of triplets, quint = quintet, sext = sextet, sept = septet, m

= multiplet, and bs = broad signal. Compounds were named following IUPAC rules. HPLC analysis: all target compounds (i.e., assessed in biological assays) were ≥ 95% pure by HPLC, confirmed via UV detection (λ = 254 nm). Analytical reversed-phase HPLC was conducted using a Kinetex EVO C18 column (5 μm, 150 mm × 4.6 mm, Phenomenex, Inc.). Compounds **10a-d**, **11a-d**, **16a-d**, **17a-d** and **76-77** were analysed by using the following method "A": eluent A, water; eluent B, CH_3CN; after 5 min at 25% B, a gradient was formed from 25% to 75% of B in 5 min and held at 75% of B for 10 min; flow rate was 1 mL/min. Compounds **12a-d**, **13a-d**, **14a-g** and **15a-d** (more lipophilic compounds, due to the long alkyl chain of the ketoxime moiety) were analysed by using the following method "B": eluent A, water; eluent B, CH_3CN; after 4 min at 30% B, a gradient was formed from 30% to 75% of B in 3 min and held at 75% of B for 3 min; then a gradient was formed from 75% to 95% of B in 3 min and held at 95% of B for 12 min; flow rate was 1 mL/min. Yields refer to isolated and purified products derived from nonoptimized procedures. CAY10499 (**2**) was purchased from Cayman Chemical and (4-(4-chlorobenzoyl)piperidin-1-yl)(3-hydroxyphenyl)methanone **6** was synthesized as previously reported.[17] Elemental analysis was used to further characterize the final compounds. Analytical results are within ± 0.4 % of the theoretical values.

*4.1.1. General procedure for the synthesis of compounds **24-29**, **60-61** and **71**.*

Thionyl chloride (10 eq) was added dropwise at 0 °C to the appropriate aliphatic carboxylic acid **18-23** (1.0 g, 1 eq). After addition was complete, the ice bath was removed, and the reaction mixture was stirred at 95 °C for 3 h under argon atmosphere. The mixture was cooled to room temperature and then evaporated to give the corresponding acid chloride that was immediately used in the next step without further purification. Aromatic acid chlorides **58**, **59** and **70** were commercially available and were used as purchased without further purification. 4-Bromoanisole (0.87 mL, 1 eq) was dissolved in anhydrous 1,2-dichloroethane (3.2 mL), cooled in an ice bath and then aluminium trichloride (1.4 eq) was added. Finally, a previously prepared solution of the acid chloride (1 eq) in anhydrous 1,2-dichloroethane (5.3 mL) was added and the resulting mixture was heated at 65 °C for 2 h. The reaction mixture was allowed to cool to room temperature, poured carefully in ice and then repeatedly

extracted with EtOAc. The combined organic phase was washed with brine and then dried over Na_2SO_4, filtered and concentrated under reduced pressure to obtain a residue that was purified by flash chromatography to afford the title compounds.

1-(5-Bromo-2-hydroxyphenyl)pentan-1-one (**24**). Yellow oil, yield: 42% from valeric acid **18** (eluent: petroleum ether). ^{1}H-NMR ($CDCl_3$) δ (ppm): 0.97 (t, 3H, *J* = 7.3 Hz), 1.43 (sext, 2H, *J* = 7.4 Hz), 1.73 (quint, 2H, *J* = 7.5 Hz), 2.97 (t, 2H, *J* = 7.4 Hz), 6.90 (d, 1H, *J* = 8.9 Hz), 7.53 (dd, 1H, *J* = 8.9, 2.4 Hz), 7.86 (d, 1H, *J* = 2.4 Hz), 12.31 (exchangeable s, 1H).

1-(5-Bromo-2-hydroxyphenyl)octan-1-one (**25**). Yellow solid, yield: 62% from ottanoic acid **19** (eluent: petroleum ether). ^{1}H-NMR ($CDCl_3$) δ (ppm): 0.89 (t, 3H, *J* = 7.2 Hz), 1.20-1.48 (m, 8H), 1.74 (quint, 2H, *J* = 7.3 Hz), 2.96 (t, 2H, *J* = 7.4 Hz), 6.89 (d, 1H, *J* = 8.9 Hz), 7.53 (dd, 1H, *J* = 8.9, 2.4 Hz), 7.86 (d, 1H, *J* = 2.4 Hz), 12.31 (exchangeable s, 1H).

1-(5-bromo-2-hydroxyphenyl)decan-1-one (**26**). White solid, yield: 45% from decanoic acid **20** (eluent: petroleum ether). ^{1}H-NMR ($CDCl_3$) δ (ppm): 0.88 (t, 3H, *J* = 6.9 Hz), 1.20-1.44 (m, 12H), 1.73 (quint, 2H, *J* = 7.4 Hz), 2.95 (t, 2H, *J* = 7.4 Hz), 6.89 (d, 1H, *J* = 8.9 Hz), 7.53 (dd, 1H, *J* = 8.9, 2.5 Hz), 7.86 (d, 1H, *J* = 2.5 Hz), 12.31 (exchangeable s, 1H).

1-(5-Bromo-2-hydroxyphenyl)dodecan-1-one (**27**). White solid, yield: 34% from dodecanoic acid **21** (eluent: petroleum ether). ^{1}H-NMR ($CDCl_3$) δ (ppm): 0.88 (t, 3H, *J* = 6.9 Hz), 1.19-1.45 (m, 16H), 1.73 (quint, 2H, *J* = 7.4 Hz), 2.95 (t, 2H, *J* = 7.4 Hz), 6.89 (d, 1H, *J* = 8.9 Hz), 7.53 (dd, 1H, *J* = 8.9, 2.4 Hz), 7.86 (d, 1H, *J* = 2.4 Hz), 12.31 (exchangeable s, 1H).

1-(5-Bromo-2-hydroxyphenyl)tetradecan-1-one (**28**). White solid, yield: 52% from myristic acid **22** (eluent: petroleum ether). ^{1}H-NMR ($CDCl_3$) δ (ppm): 0.88 (t, 3H, *J* = 6.8 Hz), 1.20-1.44 (m, 20H), 1.73 (quint, 2H, *J* = 7.4 Hz), 2.95 (t, 2H, *J* = 7.4 Hz), 6.89 (d, 1H, *J* = 8.9 Hz), 7.53 (dd, 1H, *J* = 8.9, 2.4 Hz), 7.86 (d, 1H, *J* = 2.4 Hz), 12.30 (exchangeable s, 1H).

1-(5-Bromo-2-hydroxyphenyl)hexadecan-1-one (**29**). White solid, yield: 39% from palmitic acid **23** (eluent: petroleum ether). ^{1}H-NMR ($CDCl_3$) δ (ppm): 0.88 (t, 3H, *J* = 6.7 Hz), 1.20-1.44 (m, 24H),

1.73 (quint, 2H, *J* = 7.3 Hz), 2.95 (t, 2H, *J* = 7.4 Hz), 6.89 (d, 1H, *J* = 8.9 Hz), 7.53 (dd, 1H, *J* = 8.9, 2.4 Hz), 7.86 (d, 1H, *J* = 2.5 Hz), 12.31 (exchangeable s, 1H).

(5-Bromo-2-hydroxyphenyl)(phenyl)methanone (**60**). White solid, yield: 60% from benzoyl chloride **58** (eluent: petroleum ether). ^{1}H-NMR ($CDCl_3$) δ (ppm): 6.99 (d, 1H, *J* = 9.2 Hz), 7.49-7.72 (m, 7H), 11.92 (exchangeable s, 1H).

1-(5-Bromo-2-hydroxyphenyl)-2-phenylethanone (**61**). White solid, yield: 71% from phenacetyl chloride **59** (eluent: petroleum ether/EtOAc 99:1). ^{1}H-NMR ($CDCl_3$) δ (ppm): 4.28 (s, 2H), 6.90 (d, 1H, *J* = 8.9 Hz), 7.23-7.40 (m, 5H), 7.55 (dd, 1H, *J* = 8.9, 2.4 Hz), 7.97 (d, 1H, *J* = 2.4 Hz), 12.11 (exchangeable s, 1H).

1-(5-Bromo-2-hydroxyphenyl)-2-methylpropan-1-one (**71**). Light yellow oil, yield: 36% from isobutyryl chloride **70** (eluent: petroleum ether). ^{1}H-NMR ($CDCl_3$) δ (ppm): 1.25 (d, 6H, *J* = 6.8 Hz), 3.54 (sept, 1H, *J* = 6.8 Hz), 6.91 (d, 1H, *J* = 8.9 Hz), 7.54 (dd, 1H, *J* = 8.9, 2.4 Hz), 7.88 (d, 1H, *J* = 2.5 Hz), 12.42 (exchangeable s, 1H).

*4.1.2. General procedure for the synthesis of compounds **30-44**, **62-65** and **72-73**.*

A solution of $Pd(OAc)_2$ (0.03 eq) and triphenylphosphine (0.12 eq) in ethanol (0.9 mL/0.90 mmol bromo-derivative) and toluene (0.9 mL/0.90 mmol bromo-derivative) was stirred at room temperature under argon for 10 minutes. After that period, bromo-substituted derivative **24-29**, **60-61**, **71** (320 mg, 1 eq), 2M aqueous Na_2CO_3 (0.9 mL/0.90 mmol bromo-derivative) and the appropriate substituted phenylboronic acid (1.3 eq) were sequentially added. The resulting mixture was heated at 100 °C in a sealed vial under nitrogen for 24 h. After being cooled to room temperature, the mixture was diluted with water and extracted with EtOAc. The combined organic phase was dried and concentrated. The crude product was purified by flash chromatography using the indicated eluent and pure fractions containing the desired compound were evaporated to dryness affording the desired product.

1-(3'-Fluoro-4-hydroxy-4'-methoxy-[1,1'-biphenyl]-3-yl)pentan-1-one (**30**). Yellow solid, yield: 62% from **24** and 3-fluoro-4-methoxyphenylboronic acid (eluent: *n*-hexane/EtOAc 98:2). ^{1}H-NMR ($CDCl_3$) δ (ppm): 0.98 (t, 3H, *J* = 7.3 Hz), 1.45 (sext, 2H, *J* = 7.5 Hz), 1.76 (quint, 2H, *J* = 7.5 Hz),

3.06 (t, 2H, J = 7.4 Hz), 3.94 (s, 3H), 7.05 (d, 1H, J = 8.7 Hz), 7.21-7.29 (m, 3H), 7.63 (dd, 1H, J = 8.6, 2.3 Hz), 7.87 (d, 1H, J = 2.3 Hz), 12.40 (exchangeable s, 1H).

1-(4-Hydroxy-4'-methoxy-[1,1'-biphenyl]-3-yl)pentan-1-one (**31**). White solid, yield: 69% from **24** and 4-methoxyphenylboronic acid (eluent: petroleum ether/EtOAc 98:2). ^{1}H-NMR ($CDCl_3$) δ (ppm): 0.98 (t, 3H, J = 7.4 Hz), 1.44 (sext, 2H, J = 7.5 Hz), 1.76 (quint, 2H, J = 7.5 Hz), 3.05 (t, 2H, J = 7.4 Hz), 3.86 (s, 3H), 6.99 (AA'XX', 2H, J_{AX} = 8.8 Hz, $J_{AA'/XX'}$ = 2.6 Hz), 7.04 (d, 1H, J = 8.6 Hz), 7.46 (AA'XX', 2H, J_{AX} = 8.9 Hz, $J_{AA'/XX'}$ = 2.7 Hz), 7.65 (dd, 1H, J = 8.6, 2.3 Hz), 7.89 (d, 1H, J = 2.3 Hz), 12.37 (exchangeable s, 1H).

1-(3'-Fluoro-4-hydroxy-4'-methoxy-[1,1'-biphenyl]-3-yl)octan-1-one (**32**). Light-yellow solid, yield: 61% from **25** and 3-fluoro-4-methoxyphenylboronic acid (eluent: *n*-hexane/EtOAc 98:2). ^{1}H-NMR ($CDCl_3$) δ (ppm): 0.89 (t, 3H, J = 6.9 Hz), 1.20-1.50 (m, 8H), 1.77 (quint, 2H, J = 7.4 Hz), 3.05 (t, 2H, J = 7.5 Hz), 3.94 (s, 3H), 7.00-7.07 (m, 2H), 7.21-7.30 (m, 2H), 7.63 (dd, 1H, J = 8.6, 2.3 Hz), 7.86 (d, 1H, J = 2.3 Hz), 12.40 (exchangeable s, 1H).

1-(4-Hydroxy-4'-methoxy-[1,1'-biphenyl]-3-yl)octan-1-one (**33**). Off-white solid, yield: 46% from **25** and 4-methoxyphenylboronic acid (eluent: *n*-hexane/EtOAc 98:2). ^{1}H-NMR ($CDCl_3$) δ (ppm): 0.89 (t, 3H, J = 6.9 Hz), 1.20-1.45 (m, 8H), 1.77 (quint, 2H, J = 7.5 Hz), 3.04 (t, 2H, J = 7.4 Hz), 3.86 (s, 3H), 6.99 (AA'XX', 2H, J_{AX} = 8.8 Hz, $J_{AA'/XX'}$ = 2.6 Hz), 7.04 (d, 1H, J = 8.6 Hz), 7.46 (AA'XX', 2H, J_{AX} = 8.8 Hz, $J_{AA'/XX'}$ = 2.6 Hz), 7.65 (dd, 1H, J = 8.6, 2.3 Hz), 7.88 (d, 1H, J = 2.3 Hz), 12.37 (exchangeable s, 1H).

1-(3'-Fluoro-4-hydroxy-4'-methoxy-[1,1'-biphenyl]-3-yl)decan-1-one (**34**). Off-white solid, yield: 72% from **26** and 3-fluoro-4-methoxyphenylboronic acid (eluent: *n*-hexane/EtOAc 98:2). ^{1}H-NMR ($CDCl_3$) δ (ppm): 0.88 (t, 3H, J = 6.9 Hz), 1.19-1.46 (m, 12H), 1.77 (quint, 2H, J = 7.4 Hz), 3.05 (t, 2H, J = 7.4 Hz), 3.94 (s, 3H), 7.00-7.07 (m, 2H), 7.21-7.30 (m, 2H), 7.63 (dd, 1H, J = 8.6, 2.3 Hz), 7.86 (d, 1H, J = 2.3 Hz), 12.40 (exchangeable s, 1H).

1-(4-Hydroxy-4'-methoxy-[1,1'-biphenyl]-3-yl)decan-1-one (**35**). White solid, yield: 77% from **26** and 4-methoxyphenylboronic acid (eluent: *n*-hexane/EtOAc 98:2). ^{1}H-NMR ($CDCl_3$) δ (ppm): 0.88

(t, 3H, J = 6.9 Hz), 1.19-1.46 (m, 12H), 1.77 (quint, 2H, J = 7.4 Hz), 3.04 (t, 2H, J = 7.4 Hz), 3.86 (s, 3H), 6.99 (AA'XX', 2H, J_{AX} = 8.8 Hz, $J_{AA'/XX'}$ = 2.6 Hz), 7.04 (d, 1H, J = 8.6 Hz), 7.46 (AA'XX', 2H, J_{AX} = 8.8 Hz, $J_{AA'/XX'}$ = 2.6 Hz), 7.65 (dd, 1H, J = 8.6, 2.3 Hz), 7.88 (d, 1H, J = 2.3 Hz), 12.37 (exchangeable s, 1H).

1-(3'-Fluoro-4-hydroxy-4'-methoxy-[1,1'-biphenyl]-3-yl)dodecan-1-one (**36**). Off-white solid, yield: 71% from **27** and 3-fluoro-4-methoxyphenylboronic acid (eluent: *n*-hexane/EtOAc 98:2). ^{1}H-NMR ($CDCl_3$) δ (ppm): 0.88 (t, 3H, J = 6.9 Hz), 1.19-1.46 (m, 16H), 1.77 (quint, 2H, J = 7.5 Hz), 3.05 (t, 2H, J = 7.4 Hz), 3.94 (s, 3H), 7.00-7.07 (m, 2H), 7.21-7.30 (m, 2H), 7.63 (dd, 1H, J = 8.7, 2.2 Hz), 7.86 (d, 1H, J = 2.3 Hz), 12.40 (exchangeable s, 1H).

1-(4-Hydroxy-4'-methoxy-[1,1'-biphenyl]-3-yl)dodecan-1-one (**37**). Off-white solid, yield: 64% from **27** and 4-methoxyphenylboronic acid (eluent: *n*-hexane/EtOAc 98:2). ^{1}H-NMR ($CDCl_3$) δ (ppm): 0.88 (t, 3H, J = 6.9 Hz), 1.19-1.46 (m, 16H), 1.77 (quint, 2H, J = 7.5 Hz), 3.04 (t, 2H, J = 7.4 Hz), 3.86 (s, 3H), 6.99 (AA'XX', 2H, J_{AX} = 8.8 Hz, $J_{AA'/XX'}$ = 2.6 Hz), 7.04 (d, 1H, J = 8.6 Hz), 7.46 (AA'XX', 2H, J_{AX} = 8.8 Hz, $J_{AA'/XX'}$ = 2.6 Hz), 7.65 (dd, 1H, J = 8.6, 2.3 Hz), 7.88 (d, 1H, J = 2.2 Hz), 12.37 (exchangeable s, 1H).

1-(3'-Fluoro-4-hydroxy-4'-methoxy-[1,1'-biphenyl]-3-yl)tetradecan-1-one (**38**). Off-white solid, yield: 77% from **28** and 3-fluoro-4-methoxyphenylboronic acid (eluent: petroleum ether/EtOAc 98:2). ^{1}H-NMR ($CDCl_3$) δ (ppm): 0.88 (t, 3H, J = 6.9 Hz), 1.20-1.46 (m, 20H), 1.77 (quint, 2H, J = 7.4 Hz), 3.05 (t, 2H, J = 7.4 Hz), 3.94 (s, 3H), 7.00-7.07 (m, 2H), 7.21-7.30 (m, 2H), 7.63 (dd, 1H, J = 8.7, 2.3 Hz), 7.86 (d, 1H, J = 2.3 Hz), 12.40 (exchangeable s, 1H).

1-(4-Hydroxy-4'-methoxy-[1,1'-biphenyl]-3-yl)tetradecan-1-one (**39**). White solid, yield: 81% from **28** and 4-methoxyphenylboronic acid (eluent: petroleum ether/EtOAc 98:2). ^{1}H-NMR ($CDCl_3$) δ (ppm): 0.88 (t, 3H, J = 6.9 Hz), 1.20-1.45 (m, 20H), 1.77 (quint, 2H, J = 7.3 Hz), 3.04 (t, 2H, J = 7.5 Hz), 3.86 (s, 3H), 6.99 (AA'XX', 2H, J_{AX} = 8.8 Hz, $J_{AA'/XX'}$ = 2.6 Hz), 7.04 (d, 1H, J = 8.6 Hz), 7.46 (AA'XX', 2H, J_{AX} = 8.9 Hz, $J_{AA'/XX'}$ = 2.6 Hz), 7.65 (dd, 1H, J = 8.7, 2.3 Hz), 7.88 (d, 1H, J = 2.2 Hz), 12.36 (exchangeable s, 1H).

1-(3'-Fluoro-4-hydroxy-4'-methoxy-[1,1'-biphenyl]-3-yl)hexadecan-1-one (**40**). Off-white solid, yield: 77% from **29** and 3-fluoro-4-methoxyphenylboronic acid (eluent: petroleum ether/EtOAc 98:2). ^{1}H-NMR ($CDCl_3$) δ (ppm): 0.88 (t, 3H, *J* = 6.7 Hz), 1.20-1.45 (m, 24H), 1.77 (quint, 2H, *J* = 7.4 Hz), 3.05 (t, 2H, *J* = 7.4 Hz), 3.94 (s, 3H), 7.00-7.08 (m, 2H), 7.21-7.30 (m, 2H), 7.63 (dd, 1H, *J* = 8.7, 2.3 Hz), 7.86 (d, 1H, *J* = 2.3 Hz), 12.40 (exchangeable s, 1H).

1-(4-Hydroxy-4'-methoxy-[1,1'-biphenyl]-3-yl)hexadecan-1-one (**41**). White solid, yield: 84% from **29** and 4-methoxyphenylboronic acid (eluent: petroleum ether/EtOAc 99:1). ^{1}H-NMR ($CDCl_3$) δ (ppm): 0.88 (t, 3H, *J* = 6.8 Hz), 1.20-1.45 (m, 24H), 1.77 (quint, 2H, *J* = 7.4 Hz), 3.04 (t, 2H, *J* = 7.4 Hz), 3.86 (s, 3H), 6.99 (AA'XX', 2H, J_{AX} = 8.8 Hz, $J_{AA'/XX'}$ = 2.6 Hz), 7.04 (d, 1H, *J* = 8.6 Hz), 7.46 (AA'XX', 2H, J_{AX} = 8.8 Hz, $J_{AA'/XX'}$ = 2.5 Hz), 7.65 (dd, 1H, *J* = 8.7, 2.2 Hz), 7.88 (d, 1H, *J* = 2.3 Hz), 12.36 (exchangeable s, 1H).

1-(4-Hydroxy-[1,1'-biphenyl]-3-yl)tetradecan-1-one (**42**). Off-white solid, yield: 43% from **28** and phenylboronic acid (eluent: petroleum ether/EtOAc 98:2). ^{1}H-NMR ($CDCl_3$) δ (ppm): 0.88 (t, 3H, *J* = 6.8 Hz), 1.19-1.46 (m, 20H), 1.77 (quint, 2H, *J* = 7.4 Hz), 3.05 (t, 2H, *J* = 7.4 Hz), 7.07 (d, 1H, *J* = 8.6 Hz), 7.36 (tt, 1H, *J* = 7.3, 1.5 Hz), 7.41-7.49 (m, 2H), 7.51-7.56 (m, 2H), 7.70 (dd, 1H, *J* = 8.6, 2.3 Hz), 7.94 (d, 1H, *J* = 2.2 Hz), 12.42 (exchangeable s, 1H).

1-(3'-Fluoro-4-hydroxy-[1,1'-biphenyl]-3-yl)tetradecan-1-one (**43**). Off-white solid, yield: 39% from **28** and 3-fluorophenylboronic acid (eluent: petroleum ether/EtOAc 98:2). ^{1}H-NMR ($CDCl_3$) δ (ppm): 0.88 (t, 3H, *J* = 6.8 Hz), 1.18-1.46 (m, 20H), 1.78 (quint, 2H, *J* = 7.4 Hz), 3.06 (t, 2H, *J* = 7.4 Hz), 7.05 (dddd, 1H, *J* = 11.8, 8.4, 2.5, 1.0 Hz), 7.07 (d, 1H, *J* = 8.7 Hz), 7.20-7.25 (m, 1H), 7.31 (ddd, 1H, *J* = 7.8, 1.6, 1.0 Hz), 7.37-7.46 (m, 1H), 7.68 (dd, 1H, *J* = 8.6, 2.3 Hz), 7.93 (d, 1H, *J* = 2.3 Hz), 12.45 (exchangeable s, 1H).

1-(4-Hydroxy-3'-methoxy-[1,1'-biphenyl]-3-yl)tetradecan-1-one (**44**). White solid, yield: 52% from **28** and 3-methoxyphenylboronic acid (eluent: petroleum ether/EtOAc 98:2). ^{1}H-NMR ($CDCl_3$) δ (ppm): 0.88 (t, 3H, *J* = 6.9 Hz), 1.18-1.46 (m, 20H), 1.77 (quint, 2H, *J* = 7.4 Hz), 3.05 (t, 2H, *J* = 7.4

Hz), 3.88 (s, 3H), 6.87-6.93 (m, 1H), 7.03-7.08 (m, 2H), 7.12 (ddd, 1H, *J* = 7.6, 1.8, 0.9 Hz), 7.37 (t, 1H, *J* = 7.9 Hz), 7.69 (dd, 1H, *J* = 8.7, 2.2 Hz), 7.94 (d, 1H, *J* = 2.2 Hz), 12.42 (exchangeable s, 1H).

(3'-Fluoro-4-hydroxy-4'-methoxy-[1,1'-biphenyl]-3-yl)(phenyl)methanone (**62**). Yellow solid, yield: 78% from **60** and 3-fluoro-4-methoxyphenylboronic acid (eluent: petroleum ether/EtOAc 98:2). ^{1}H-NMR ($CDCl_3$) δ (ppm): 3.90 (s, 3H), 6.98 (t, 1H, *J* = 8.8 Hz), 7.12-7.20 (m, 3H), 7.50-7.57 (m, 2H), 7.62 (tt, 1H, *J* = 7.4, 1.6 Hz), 7.69 (dd, 1H, *J* = 8.6, 2.4 Hz), 7.71-7.75 (m, 3H), 11.97 (exchangeable s, 1H).

(4-Hydroxy-4'-methoxy-[1,1'-biphenyl]-3-yl)(phenyl)methanone (**63**). Yellow solid, yield: 78% from **60** and 4-methoxyphenylboronic acid (eluent: petroleum ether/EtOAc 98:2). ^{1}H-NMR ($CDCl_3$) δ (ppm): 3.83 (s, 3H), 6.93 (AA'XX', 2H, J_{AX} = 8.8 Hz, $J_{AA'/XX'}$ = 2.6 Hz), 7.14 (d, 1H, *J* = 8.6 Hz), 7.38 (AA'XX', 2H, J_{AX} = 8.8 Hz, $J_{AA'/XX'}$ = 2.6 Hz), 7.49-7.56 (m, 2H), 7.61 (tt, 1H, *J* = 7.5, 1.7 Hz), 7.69-7.76 (m, 4H), 11.96 (exchangeable s, 1H).

1-(3'-Fluoro-4-hydroxy-4'-methoxy-[1,1'-biphenyl]-3-yl)-2-phenylethanone (**64**). Yellow solid, yield: 82% from **61** and 3-fluoro-4-methoxyphenylboronic acid (eluent: petroleum ether/EtOAc 95:5). ^{1}H-NMR ($CDCl_3$) δ (ppm): 3.94 (s, 3H), 4.36 (s, 2H), 7.03 (t, 1H, *J* = 8.8 Hz), 7.05 (d, 1H, *J* = 8.7 Hz), 7.16-7.24 (m, 2H), 7.27-7.41 (m, 5H), 7.63 (dd, 1H, *J* = 8.7, 2.3 Hz), 7.97 (d, 1H, *J* = 2.3 Hz), 12.19 (exchangeable s, 1H).

1-(4-Hydroxy-4'-methoxy-[1,1'-biphenyl]-3-yl)-2-phenylethanone (**65**). Yellow solid, yield: 79% from **61** and 4-methoxyphenylboronic acid (eluent: petroleum ether/EtOAc 95:5). ^{1}H-NMR ($CDCl_3$) δ (ppm): 3.86 (s, 3H), 4.37 (s, 2H), 6.99 (AA'XX', 2H, J_{AX} = 8.8 Hz, $J_{AA'/XX'}$ = 2.6 Hz), 7.05 (d, 1H, *J* = 8.7 Hz), 7.27-7.33 (m, 3H), 7.34-7.40 (m, 2H), 7.42 (AA'XX', 2H, J_{AX} = 8.9 Hz, $J_{AA'/XX'}$ = 2.6 Hz), 7.66 (dd, 1H, *J* = 8.6, 2.3 Hz), 8.00 (d, 1H, *J* = 2.2 Hz), 12.16 (exchangeable s, 1H).

1-(3'-Fluoro-4-hydroxy-4'-methoxy-[1,1'-biphenyl]-3-yl)-2-methylpropan-1-one (**72**). Yellow solid, yield: 66% from **71** and 3-fluoro-4-methoxyphenylboronic acid (eluent: petroleum ether/EtOAc 99:1). ^{1}H-NMR ($CDCl_3$) δ (ppm): 1.29 (d, 6H, *J* = 6.8 Hz), 3.69 (sept, 1H, *J* = 6.8 Hz), 3.94 (s, 3H),

6.98-7.09 (m, 2H), 7.21-7.30 (m, 2H), 7.64 (dd, 1H, *J* = 8.7, 2.3 Hz), 7.89 (d, 1H, *J* = 2.3 Hz), 12.51 (exchangeable s, 1H).

1-(4-Hydroxy-4'-methoxy-[1,1'-biphenyl]-3-yl)-2-methylpropan-1-one (**73**). Yellow solid, yield: 66% from **71** and 4-methoxyphenylboronic acid (eluent: petroleum ether/EtOAc 99:1). ^{1}H-NMR ($CDCl_3$) δ (ppm): 1.28 (d, 6H, *J* = 6.8 Hz), 3.70 (sept, 1H, *J* = 6.8 Hz), 3.86 (s, 3H), 6.99 (AA'XX', 2H, J_{AX} = 8.8 Hz, $J_{AA'/XX'}$ = 2.6 Hz), 7.06 (d, 1H, *J* = 8.7 Hz), 7.46 (AA'XX', 2H, J_{AX} = 8.8 Hz, $J_{AA'/XX'}$ = 2.6 Hz), 7.66 (dd, 1H, *J* = 8.6, 2.2 Hz), 7.91 (d, 1H, *J* = 2.3 Hz), 12.47 (exchangeable s, 1H).

*4.1.3. General procedure for the synthesis of compounds **45-57**, **66-69** and **74-75**.*

A solution of methoxylated intermediate **30-41**, **44**, **62-65**, **72-73** (200 mg, 1 eq) in anhydrous CH_2Cl_2 (6.8 mL) was cooled to −10 °C and treated dropwise with a 1.0 M solution of BBr_3 in CH_2Cl_2 (1.8 mL) under argon. The mixture was left under stirring at the same temperature for 5 minutes and then at 0 °C for 1 h and finally at room temperature until starting material was consumed (TLC). The mixture was then diluted with water and extracted with ethyl acetate. The organic phase was washed with brine, dried, and concentrated. The crude product was purified by flash chromatography over silica gel to afford the desired compounds.

1-(3',4-Dihydroxy-[1,1'-biphenyl]-3-yl)tetradecan-1-one (**45**). Yellow solid, yield: 79% from **44** (eluent: *n*-hexane/EtOAc 9:1). ^{1}H-NMR ($CDCl_3$) δ (ppm): 0.88 (t, 3H, *J* = 6.6 Hz), 1.18-1.46 (m, 20H), 1.77 (quint, 2H, *J* = 7.4 Hz), 3.05 (t, 2H, *J* = 7.4 Hz), 4.86 (exchangeable bs, 1H), 6.82 (ddd, 1H, *J* = 8.1, 2.5, 0.9 Hz), 7.01 (t, 1H, *J* = 2.1 Hz), 7.06 (d, 1H, *J* = 8.6 Hz), 7.11 (ddd, 1H, *J* = 7.7, 1.7, 0.9 Hz), 7.32 (t, 1H, *J* = 7.9 Hz), 7.68 (dd, 1H, *J* = 8.6, 2.2 Hz), 7.93 (d, 1H, *J* = 2.2 Hz), 12.43 (exchangeable s, 1H).

1-(3'-Fluoro-4,4'-dihydroxy-[1,1'-biphenyl]-3-yl)pentan-1-one (**46**). Off-white solid, yield: 85% from **30** (eluent: *n*-hexane/EtOAc 9:1). ^{1}H-NMR ($CDCl_3$) δ (ppm): 0.98 (t, 3H, *J* = 7.3 Hz), 1.45 (sext, 2H, *J* = 7.5 Hz), 1.76 (quint, 2H, *J* = 7.5 Hz), 3.05 (t, 2H, *J* = 7.4 Hz), 7.05 (d, 1H, *J* = 8.6 Hz), 7.08 (t,

1H, J = 8.3 Hz), 7.20 (ddd, 1H, J = 8.3, 2.2, 1.0 Hz), 7.25 (dd, 1H, J = 11.6, 2.1 Hz), 7.62 (dd, 1H, J = 8.7, 2.3 Hz), 7.86 (d, 1H, J = 2.3 Hz), 12.40 (exchangeable s, 1H).

1-(4,4'-Dihydroxy-[1,1'-biphenyl]-3-yl)pentan-1-one (**47**). Yellow solid, yield: 99% from **31** (eluent: petroleum ether/EtOAc 9:1). ^{1}H-NMR ($CDCl_3$) δ (ppm): 0.98 (t, 3H, J = 7.3 Hz), 1.44 (sext, 2H, J = 7.5 Hz), 1.76 (quint, 2H, J = 7.5 Hz), 3.05 (t, 2H, J = 7.4 Hz), 4.89 (exchangeable bs, 1H), 6.92 (AA'XX', 2H, J_{AX} = 8.7 Hz, $J_{AA'/XX'}$ = 2.6 Hz), 7.04 (d, 1H, J = 8.6 Hz), 7.41 (AA'XX', 2H, J_{AX} = 8.7 Hz, $J_{AA'/XX'}$ = 2.6 Hz), 7.64 (dd, 1H, J = 8.6, 2.3 Hz),7.88 (d, 1H, J = 2.3 Hz), 12.38 (exchangeable s, 1H).

1-(3'-Fluoro-4,4'-dihydroxy-[1,1'-biphenyl]-3-yl)octan-1-one (**48**). Yellow solid, yield: 85% from **32** (eluent: *n*-hexane/EtOAc 9:1). ^{1}H-NMR ($CDCl_3$) δ (ppm): 0.89 (t, 3H, J = 6.9 Hz), 1.23-1.46 (m, 8H), 1.77 (quint, 2H, J = 7.4 Hz), 3.05 (t, 2H, J = 7.4 Hz), 5.16 (exchangeable d, 1H, J = 3.8 Hz), 7.02-7.12 (m, 2H), 7.20 (ddd, 1H, J = 8.4, 2.2, 1.0 Hz), 7.25 (dd, 1H, J = 11.6, 2.1 Hz), 7.62 (dd, 1H, J = 8.7, 2.3 Hz), 7.85 (d, 1H, J = 2.3 Hz), 12.40 (exchangeable s, 1H).

1-(4,4'-Dihydroxy-[1,1'-biphenyl]-3-yl)octan-1-one (**49**). Yellow solid, yield: 92% from **33** (eluent: *n*-hexane/EtOAc 9:1). ^{1}H-NMR ($CDCl_3$) δ (ppm): 0.89 (t, 3H, J = 6.9 Hz), 1.22-1.45 (m, 8H), 1.77 (quint, 2H, J = 7.4 Hz), 3.04 (t, 2H, J = 7.4 Hz), 4.87 (exchangeable bs, 1H), 6.92 (AA'XX', 2H, J_{AX} = 8.7 Hz, $J_{AA'/XX'}$ = 2.6 Hz), 7.04 (d, 1H, J = 8.6 Hz), 7.41 (AA'XX', 2H, J_{AX} = 8.8 Hz, $J_{AA'/XX'}$ = 2.6 Hz), 7.64 (dd, 1H, J = 8.7, 2.2 Hz), 7.87 (d, 1H, J = 2.2 Hz), 12.37 (exchangeable s, 1H).

1-(3'-Fluoro-4,4'-dihydroxy-[1,1'-biphenyl]-3-yl)decan-1-one (**50**). Yellow solid, yield: 82% from **34** (eluent: *n*-hexane/EtOAc 9:1). ^{1}H-NMR ($CDCl_3$) δ (ppm): 0.88 (t, 3H, J = 6.9 Hz), 1.19-1.46 (m, 12H), 1.77 (quint, 2H, J = 7.4 Hz), 3.04 (t, 2H, J = 7.4 Hz), 5.20 (exchangeable bs, 1H), 7.02-7.11 (m, 2H), 7.20 (ddd, 1H, J = 8.4, 2.2, 1.0 Hz), 7.25 (dd, 1H, J = 11.6, 2.2 Hz), 7.62 (dd, 1H, J = 8.6, 2.3 Hz), 7.86 (d, 1H, J = 2.3 Hz), 12.40 (exchangeable s, 1H).

1-(4,4'-Dihydroxy-[1,1'-biphenyl]-3-yl)decan-1-one (**51**). Yellow solid, yield: 99% from **35** (eluent: *n*-hexane/EtOAc 9:1). ^{1}H-NMR ($CDCl_3$) δ (ppm): 0.88 (t, 3H, J = 6.9 Hz), 1.19-1.46 (m, 12H), 1.77 (quint, 2H, J = 7.4 Hz), 3.04 (t, 2H, J = 7.4 Hz), 4.98 (exchangeable bs, 1H), 6.92 (AA'XX', 2H, J_{AX}

= 8.7 Hz, $J_{AA'/XX'}$ = 2.6 Hz), 7.04 (d, 1H, *J* = 8.6 Hz), 7.41 (AA'XX', 2H, J_{AX} = 8.7 Hz, $J_{AA'/XX'}$ = 2.6 Hz), 7.64 (dd, 1H, *J* = 8.6, 2.3 Hz), 7.88 (d, 1H, *J* = 2.3 Hz), 12.38 (exchangeable s, 1H).

1-(3'-Fluoro-4,4'-dihydroxy-[1,1'-biphenyl]-3-yl)dodecan-1-one (**52**). Yellow solid, yield: 91% from **36** (eluent: *n*-hexane/EtOAc 9:1). ^{1}H-NMR ($CDCl_3$) δ (ppm): 0.88 (t, 3H, *J* = 6.9 Hz), 1.20-1.45 (m, 16H), 1.77 (quint, 2H, *J* = 7.5 Hz), 3.05 (t, 2H, *J* = 7.4 Hz), 5.19 (exchangeable d, 1H, *J* = 4.1 Hz), 7.02-7.11 (m, 2H), 7.20 (ddd, 1H, *J* = 8.3, 2.2, 1.0 Hz), 7.26 (dd, 1H, *J* = 11.6, 2.1 Hz), 7.62 (dd, 1H, *J* = 8.6, 2.3 Hz), 7.85 (d, 1H, *J* = 2.3 Hz), 12.41 (exchangeable s, 1H).

1-(4,4'-Dihydroxy-[1,1'-biphenyl]-3-yl)dodecan-1-one (**53**). Yellow solid, yield: 91% from **37** (eluent: *n*-hexane/EtOAc 9:1). ^{1}H-NMR ($CDCl_3$) δ (ppm): 0.88 (t, 3H, *J* = 6.9 Hz), 1.19-1.45 (m, 16H), 1.77 (quint, 2H, *J* = 7.4 Hz), 3.04 (t, 2H, *J* = 7.4 Hz), 4.88 (bs, 1H), 6.92 (AA'XX', 2H, J_{AX} = 8.6 Hz, $J_{AA'/XX'}$ = 2.5 Hz), 7.04 (d, 1H, *J* = 8.6 Hz), 7.41 (AA'XX', 2H, J_{AX} = 8.7 Hz, $J_{AA'/XX'}$ = 2.5 Hz), 7.64 (dd, 1H, *J* = 8.6, 2.3 Hz), 7.87 (d, 1H, *J* = 2.3 Hz), 12.38 (exchangeable s, 1H).

1-(3'-Fluoro-4,4'-dihydroxy-[1,1'-biphenyl]-3-yl)tetradecan-1-one (**54**). Yellow solid, yield: 93% from **38** (eluent: petroleum ether/EtOAc 9:1). ^{1}H-NMR ($CDCl_3$) δ (ppm): 0.88 (t, 3H, *J* = 6.9 Hz), 1.20-1.46 (m, 20H), 1.77 (quint, 2H, *J* = 7.4 Hz), 3.04 (t, 2H, *J* = 7.4 Hz), 5.13 (exchangeable d, 1H, *J* = 4.0 Hz), 7.02-7.11 (m, 2H), 7.20 (ddd, 1H, *J* = 8.4, 2.2, 1.0 Hz), 7.26 (dd, 1H, *J* = 11.6, 2.1 Hz), 7.62 (dd, 1H, *J* = 8.6, 2.3 Hz), 7.86 (d, 1H, *J* = 2.3 Hz), 12.40 (exchangeable s, 1H).

1-(4,4'-Dihydroxy-[1,1'-biphenyl]-3-yl)tetradecan-1-one (**55**). White solid, yield: 91% from **39** (eluent: petroleum ether/EtOAc 9:1). ^{1}H-NMR ($CDCl_3$) δ (ppm): 0.88 (t, 3H, *J* = 6.9 Hz), 1.20-1.45 (m, 20H), 1.77 (quint, 2H, *J* = 7.4 Hz), 3.04 (t, 2H, *J* = 7.4 Hz), 4.83 (exchangeable bs, 1H), 6.92 (AA'XX', 2H, J_{AX} = 8.7 Hz, $J_{AA'/XX'}$ = 2.6 Hz), 7.04 (d, 1H, *J* = 8.6 Hz), 7.41 (AA'XX', 2H, J_{AX} = 8.8 Hz, $J_{AA'/XX'}$ = 2.6 Hz), 7.64 (dd, 1H, *J* = 8.6, 2.3 Hz), 7.87 (d, 1H, *J* = 2.3 Hz), 12.37 (exchangeable s, 1H).

1-(3'-Fluoro-4,4'-dihydroxy-[1,1'-biphenyl]-3-yl)hexadecan-1-one (**56**). Yellow solid, yield: 92% from **40** (eluent: petroleum ether/EtOAc 9:1). ^{1}H-NMR ($CDCl_3$) δ (ppm): 0.88 (t, 3H, *J* = 6.8 Hz), 1.20-1.46 (m, 24H), 1.77 (quint, 2H, *J* = 7.4 Hz), 3.04 (t, 2H, *J* = 7.5 Hz), 5.18 (exchangeable d, 1H,

J = 4.1 Hz), 7.03-7.11 (m, 2H), 7.20 (ddd, 1H, *J* = 8.4, 2.0, 0.9 Hz), 7.26 (dd, 1H, *J* = 11.6, 2.1 Hz), 7.62 (dd, 1H, *J* = 8.7, 2.3 Hz), 7.86 (d, 1H, *J* = 2.3 Hz), 12.40 (exchangeable s, 1H).

1-(4,4'-Dihydroxy-[1,1'-biphenyl]-3-yl)hexadecan-1-one (**57**). White solid, yield: 94% from **41** (eluent: petroleum ether/EtOAc 85:15). ^{1}H-NMR ($CDCl_3$) δ (ppm): 0.88 (t, 3H, *J* = 6.8 Hz), 1.20-1.46 (m, 24H), 1.77 (quint, 2H, *J* = 7.4 Hz), 3.04 (t, 2H, *J* = 7.4 Hz), 4.84 (exchangeable bs, 1H), 6.92 (AA'XX', 2H, J_{AX} = 8.7 Hz, $J_{AA'/XX'}$ = 2.6 Hz), 7.04 (d, 1H, *J* = 8.6 Hz), 7.41 (AA'XX', 2H, J_{AX} = 8.7 Hz, $J_{AA'/XX'}$ = 2.6 Hz), 7.64 (dd, 1H, *J* = 8.7, 2.2 Hz), 7.87 (d, 1H, *J* = 2.2 Hz), 12.36 (exchangeable s, 1H).

(3'-Fluoro-4,4'-dihydroxy-[1,1'-biphenyl]-3-yl)(phenyl)methanone (**66**). Yellow solid, yield: 95% from **62** (eluent: petroleum ether/EtOAc 9:1). ^{1}H-NMR ($CDCl_3$) δ (ppm): 5.12 (exchangeable d, 1H, *J* = 4.1 Hz), 7.02 (t, 1H, *J* = 8.7 Hz), 7.12 (ddd, 1H, *J* = 8.4, 2.2, 0.9 Hz), 7.15 (dd, 1H, *J* = 8.6, 0.3 Hz), 7.16 (dd, 1H, *J* = 11.6, 2.2 Hz), 7.51-7.57 (m, 2H), 7.63 (tt, 1H, *J* = 7.4, 1.6 Hz), 7.68 (dd, 1H, *J* = 8.5, 2.3 Hz), 7.70-7.75 (m, 3H), 11.97 (exchangeable s, 1H).

(4,4'-Dihydroxy-[1,1'-biphenyl]-3-yl)(phenyl)methanone (**67**). White solid, yield: 96% from **63** (eluent: petroleum ether/EtOAc 8:2). ^{1}H-NMR ($CDCl_3$) δ (ppm): 4.86 (exchangeable bs, 1H), 6.86 (AA'XX', 2H, J_{AX} = 8.8 Hz, $J_{AA'/XX'}$ = 2.6 Hz), 7.14 (dd, 1H, *J* = 8.6, 0.4 Hz), 7.33 (AA'XX', 2H, J_{AX} = 8.8 Hz, $J_{AA'/XX'}$ = 2.6 Hz), 7.50-7.56 (m, 2H), 7.61 (tt, 1H, *J* = 7.4, 1.7 Hz), 7.68-7.76 (m, 4H), 11.96 (exchangeable s, 1H).

1-(3'-Fluoro-4,4'-dihydroxy-[1,1'-biphenyl]-3-yl)-2-phenylethanone (**68**). Yellow solid, yield: 93% from **64** (eluent: petroleum ether/EtOAc 9:1). ^{1}H-NMR ($CDCl_3$) δ (ppm): 4.36 (s, 2H), 5.18 (exchangeable d, 1H, *J* = 4.0 Hz), 7.05 (d, 1H, *J* = 8.7 Hz), 7.07 (t, 1H, *J* = 8.6 Hz), 7.16 (ddd, 1H, *J* = 8.4, 2.2, 0.9 Hz), 7.20 (dd, 1H, *J* = 11.5, 2.1 Hz), 7.27-7.33 (m, 3H), 7.34-7.41 (m, 2H), 7.62 (dd, 1H, *J* = 8.6, 2.2 Hz), 7.96 (d, 1H, *J* = 2.3 Hz), 12.19 (exchangeable s, 1H).

1-(4,4'-Dihydroxy-[1,1'-biphenyl]-3-yl)-2-phenylethanone (**69**). Yellow solid, yield: 97% from **65** (eluent: petroleum ether/EtOAc 8:2). ^{1}H-NMR ($CDCl_3$) δ (ppm): 4.36 (s, 2H), 4.88 (exchangeable s,

1H), 6.91 (AA'XX', 2H, J_{AX} = 8.7 Hz, $J_{AA'/XX'}$ = 2.6 Hz), 7.04 (d, 1H, *J* = 8.7 Hz), 7.27-7.40 (m, 7H), 7.65 (dd, 1H, *J* = 8.6, 2.3 Hz), 7.98 (d, 1H, *J* = 2.3 Hz), 12.16 (exchangeable s, 1H).

1-(3'-Fluoro-4,4'-dihydroxy-[1,1'-biphenyl]-3-yl)-2-methylpropan-1-one (**74**). Yellow solid, yield: 77% from **72** (eluent: *n*-hexane/EtOAc 9:1). ^{1}H-NMR ($CDCl_3$) δ (ppm): 1.29 (d, 6H, *J* = 6.8 Hz), 3.69 (sept, 1H, *J* = 6.8 Hz), 5.20 (exchangeable bs, 1H), 7.04-7.10 (m, 2H), 7.20 (ddd, 1H, *J* = 8.4, 2.2, 1.0 Hz), 7.25 (dd, 1H, *J* = 11.6, 2.2 Hz), 7.62 (dd, 1H, *J* = 8.6, 2.3 Hz), 7.88 (d, 1H, *J* = 2.3 Hz), 12.51 (exchangeable s, 1H).

1-(4,4'-Dihydroxy-[1,1'-biphenyl]-3-yl)-2-methylpropan-1-one (**75**). Yellow solid, yield: 81% from **73** (eluent: *n*-hexane/EtOAc 9:1). ^{1}H-NMR ($CDCl_3$) δ (ppm): 1.28 (d, 6H, *J* = 6.8 Hz), 3.70 (sept, 1H, *J* = 7.0 Hz), 4.88 (exchangeable bs, 1H), 6.92 (AA'XX', 2H, J_{AX} = 8.7 Hz, $J_{AA'/XX'}$ = 2.5 Hz), 7.06 (d, 1H, *J* = 8.6 Hz), 7.41 (AA'XX', 2H, J_{AX} = 8.7 Hz, $J_{AA'/XX'}$ = 2.5 Hz), 7.65 (dd, 1H, *J* = 8.6, 2.2 Hz), 7.90 (d, 1H, *J* = 2.2 Hz), 12.48 (exchangeable s, 1H).

*4.1.4. General procedure for the synthesis of final compounds **10a-d**, **11a-d**. **12a-d**, **13a-d**, **14a-g**, **15a-d**, **16a-d**, **17a-d**, **76** and **77**.*

A solution of ketones **30-43**, **45-57**, **62-69**, **74-75** (100 mg, 1 eq) in ethanol (5.8 mL) was treated with solid hydroxylamine hydrochloride (6 eq) and the mixture was heated at 50 °C until the complete disappearance of the starting compound by TLC analysis had been verified. After being cooled to room temperature, part of the solvent was removed under vacuum, and the mixture was diluted with water and extracted with EtOAc. The organic phase was dried and evaporated to afford a crude residue that was purified by column chromatography to afford the desired ketoxime derivatives.

(*E*)-1-(3'-fluoro-4,4'-dihydroxy-[1,1'-biphenyl]-3-yl)pentan-1-one oxime (**10a**). Light-yellow solid, yield: 85% from **46** (eluent: *n*-hexane/EtOAc 8:2). ^{1}H-NMR (acetone-d_6) δ (ppm): 0.97 (t, 3H, *J* = 7.3 Hz), 1.49 (sext, 2H, *J* = 7.4 Hz), 1.66 (quint, 2H, *J* = 7.5 Hz), 3.04 (t, 2H, *J* = 7.8 Hz), 6.95 (d, 1H, *J* = 8.5 Hz), 7.06 (dd, 1H, *J* = 9.1, 8.4 Hz), 7.28 (ddd, 1H, *J* = 8.4, 2.2, 1.0 Hz), 7.37 (dd, 1H, *J* = 12.6, 2.2 Hz), 7.50 (dd, 1H, *J* = 8.5, 2.3 Hz), 7.72 (d, 1H, *J* = 2.2 Hz), 8.70 (exchangeable bs, 1H), 10.68 (exchangeable bs, 1H), 11.63 (exchangeable s, 1H). ^{13}C-NMR (acetone-d_6) δ (ppm): 14.13,

23.48, 24.59, 29.72, 114.77 (d, *J* = 19.1 Hz), 118.47, 118.95 (d, *J* = 3.1 Hz), 119.00, 123.33 (d, *J* = 2.9 Hz), 126.41, 129.35, 131.55 (d, *J* = 2.1 Hz), 134.00 (d, *J* = 6.6 Hz), 144.66 (d, *J* = 13.2 Hz), 152.57 (d, *J* = 239.9 Hz), 158.76, 163.17. HPLC analysis (method A): retention time = 12.339 min; peak area, 99% (254 nm). Elemental analysis for $C_{17}H_{18}FNO_3$ calculated: % C, 67.31; % H, 5.98; % N, 4.62; found: % C, 67.26; % H, 5.99; % N, 4,61.

(*E*)-1-(3'-fluoro-4-hydroxy-4'-methoxy-[1,1'-biphenyl]-3-yl)pentan-1-one oxime (**10b**). Light-yellow solid, yield: 69% from **30** (eluent: *n*-hexane/EtOAc 9:1). ^{1}H-NMR (acetone-d_6) δ (ppm): 0.97 (t, 3H, *J* = 7.3 Hz), 1.49 (sext, 2H, *J* = 7.4 Hz), 1.66 (quint, 2H, *J* = 7.7 Hz), 3.04 (t, 2H, *J* = 7.8 Hz), 3.92 (s, 3H), 6.96 (d, 1H, *J* = 8.4 Hz), 7.19 (t, 1H, *J* = 8.9 Hz), 7.36-7.44 (m, 2H), 7.52 (dd, 1H, *J* = 8.5, 2.3 Hz), 7.75 (d, 1H, *J* = 2.3 Hz), 10.70 (exchangeable s, 1H), 11.65 (exchangeable s, 1H). ^{13}C-NMR (acetone-d_6) δ (ppm): 14.16, 23.52, 24.62, 29.75, 56.61, 114.79 (d, *J* = 19.1 Hz), 114.97 (d, *J* = 2.0 Hz), 118.55, 119.02, 123.13 (d, *J* = 3.0 Hz), 126.56, 129.46, 131.31 (d, *J* = 2.0 Hz), 134.82 (d, *J* = 7.0 Hz), 147.61 (d, *J* = 11.1 Hz), 153.37 (d, *J* = 244.5 Hz), 158.95, 163.19. HPLC analysis (method A): retention time = 13.731 min; peak area, 98% (254 nm). Elemental analysis for $C_{18}H_{20}FNO_3$ calculated: % C, 68.12; % H, 6.35; % N, 4.41; found: % C, 68.24; % H, 6.34; % N, 4.40.(*E*)-1-(4,4'-dihydroxy-[1,1'-biphenyl]-3-yl)pentan-1-one oxime (**10c**). Off-white solid, yield: 90% from **47** (eluent: *n*-hexane/EtOAc 8:2). ^{1}H-NMR (acetone-d_6) δ (ppm): 0.97 (t, 3H, *J* = 7.3 Hz), 1.49 (sext, 2H, *J* = 7.4 Hz), 1.66 (quint, 2H, *J* = 7.7 Hz), 3.02 (t, 2H, *J* = 7.8 Hz), 6.90 (AA'XX', 2H, J_{AX} = 8.7 Hz, $J_{AA'/XX'}$ = 2.6 Hz), 6.93 (d, 1H, *J* = 8.4 Hz), 7.42-7.49 (m, 3H), 7.69 (d, 1H, *J* = 2.3 Hz), 8.38 (exchangeable bs, 1H), 10.66 (exchangeable bs, 1H), 11.55 (exchangeable s, 1H). ^{13}C-NMR (acetone-d_6) δ (ppm): 14.14, 23.51, 24.63, 29.74, 116.51 (2C), 118.35, 118.82, 126.23, 128.42 (2C), 129.28, 132.80, 133.01, 157.48, 158.31, 163.21. HPLC analysis (method A): retention time = 12.118 min; peak area, 99% (254 nm). Elemental analysis for $C_{17}H_{19}NO_3$ calculated: % C, 71.56; % H, 6.71; % N, 4.91; found: % C, 71.48; % H, 6.70; % N, 4.91.

(*E*)-1-(4-hydroxy-4'-methoxy-[1,1'-biphenyl]-3-yl)pentan-1-one oxime (**10d**). White solid, yield: 93% from **31** (eluent: *n*-hexane/EtOAc 9:1). ^{1}H-NMR (acetone-d_6) δ (ppm): 0.97 (t, 3H, *J* = 7.3 Hz),

1.49 (sext, 2H, J = 7.4 Hz), 1.66 (quint, 2H, J = 7.6 Hz), 3.07 (t, 2H, J = 7.9 Hz), 3.83 (s, 3H), 6.95 (d, 1H, J = 8.5 Hz), 7.00 (AA'XX', 2H, J_{AX} = 8.9 Hz, $J_{AA'/XX'}$ = 2.6 Hz), 7.49 (dd, 1H, J = 8.4, 2.3 Hz), 7.54 (AA'XX', 2H, J_{AX} = 8.9 Hz, $J_{AA'/XX'}$ = 2.6 Hz), 7.71 (d, 1H, J = 2.2 Hz), 10.67 (exchangeable s, 1H), 11.58 (exchangeable s, 1H). ^{13}C-NMR (acetone-d_6) δ (ppm): 14.10, 23.51, 24.63, 29.73, 55.56, 115.07 (2C), 118.41, 118.87, 126.36, 128.34 (2C), 129.37, 132.47, 134.02, 158.48, 159.82, 163.18. HPLC analysis (method A): retention time = 13.749 min; peak area, 97% (254 nm). Elemental analysis for $C_{18}H_{21}NO_3$ calculated: % C, 72.22; % H, 7.07; % N, 4.68; found: % C, 72.10; % H, 7.05; % N, 4.66.

(*E*)-1-(3'-fluoro-4,4'-dihydroxy-[1,1'-biphenyl]-3-yl)octan-1-one oxime (**11a**). Light-yellow solid, yield: 77% from **48** (eluent: *n*-hexane/EtOAc 85:15). ^{1}H-NMR (acetone-d_6) δ (ppm): 0.87 (t, 3H, J = 7.0 Hz), 1.23-1.43 (m, 6H), 1.48 (quint, 2H, J = 6.9 Hz), 1.68 (quint, 2H, J = 7.7 Hz), 3.03 (t, 2H, J = 7.9 Hz), 6.95 (d, 1H, J = 8.5 Hz), 7.05 (dd, 1H, J = 9.2, 8.4 Hz), 7.28 (ddd, 1H, J = 8.4, 2.2, 1.0 Hz), 7.37 (dd, 1H, J = 12.6, 2.2 Hz), 7.50 (dd, 1H, J = 8.5, 2.3 Hz), 7.72 (d, 1H, J = 2.3 Hz), 8.65 (exchangeable bs, 1H), 10.70 (exchangeable bs, 1H), 11.62 (exchangeable s, 1H). ^{13}C-NMR (acetone-d_6) δ (ppm): 14.32, 23.29, 24.80, 27.51, 29.71, 30.34, 32.49, 114.78 (d, J = 10.0 Hz), 118.49, 118.95, 118.99 (d, J = 3.6 Hz), 123.33 (d, J = 3.0 Hz), 126.44, 129.36, 131.56 (d, J = 2.2 Hz), 134.01 (d, J = 6.6 Hz), 144.68 (d, J = 13.2 Hz), 152.59 (d, J = 239.8 Hz), 158.77, 163.22. HPLC analysis (method A): retention time = 13.628 min; peak area, 99% (254 nm). Elemental analysis for $C_{20}H_{24}FNO_3$ calculated: % C, 69.55; % H, 7.00; % N, 4.06; found: % C, 69.50; % H, 7.01; % N, 4.05.

(*E*)-1-(3'-fluoro-4-hydroxy-4'-methoxy-[1,1'-biphenyl]-3-yl)octan-1-one oxime (**11b**). White solid, yield: 83% from **32** (eluent: *n*-hexane/EtOAc 9:1). ^{1}H-NMR (acetone-d_6) δ (ppm): 0.87 (t, 3H, J = 7.0 Hz), 1.24-1.43 (m, 6H), 1.48 (quint, 2H, J = 7.3 Hz), 1.68 (quint, 2H, J = 7.6 Hz), 3.04 (t, 2H, J = 7.9 Hz), 3.92 (s, 3H), 6.96 (d, 1H, J = 8.5 Hz), 7.19 (t, 1H, J = 8.9 Hz), 7.36-7.44 (m, 2H), 7.52 (dd, 1H, J = 8.5, 2.3 Hz), 7.61 (d, 1H, J = 2.3 Hz), 10.71 (exchangeable s, 1H), 11.65 (exchangeable s, 1H). ^{13}C-NMR (acetone-d_6) δ (ppm): 14.33, 23.30, 24.81, 27.52, 29.72, 30.35, 32.49, 56.59, 114.77 (d, J = 18.5 Hz), 114.93 (d, J = 2.4 Hz), 118.54, 119.00, 123.11 (d, J = 2.9 Hz), 126.55, 129.44,

131.28 (d, J = 2.1 Hz), 134.80 (d, J = 6.5 Hz), 147.58 (d, J = 10.4 Hz), 153.35 (d, J = 243.8 Hz), 158.93, 163.20. HPLC analysis (method A): retention time = 15.941 min; peak area, 99% (254 nm). Elemental analysis for $C_{21}H_{26}FNO_3$ calculated: % C, 70.17; % H, 7.29; % N, 3.90; found: % C, 70.24; % H, 7.27; % N, 3.89.

(*E*)-1-(4,4'-dihydroxy-[1,1'-biphenyl]-3-yl)octan-1-one oxime (**11c**). Light-yellow solid, yield: 59% from **49** (eluent: *n*-hexane/EtOAc 8:2). ^{1}H-NMR (acetone-d_6) δ (ppm): 0.87 (t, 3H, J = 7.0 Hz), 1.24-1.43 (m, 6H), 1.48 (quint, 2H, J = 7.3 Hz), 1.68 (quint, 2H, J = 7.7 Hz), 3.02 (t, 2H, J = 7.9 Hz), 6.90 (AA'XX', 2H, J_{AX} = 8.8 Hz, $J_{AA'/XX'}$ = 2.6 Hz), 6.93 (d, 1H, J = 8.4 Hz), 7.42-7.49 (m, 3H), 7.69 (d, 1H, J = 2.3 Hz), 8.37 (exchangeable bs, 1H), 10.66 (exchangeable bs, 1H), 11.55 (exchangeable s, 1H). ^{13}C-NMR (acetone-d_6) δ (ppm): 14.34, 23.29, 24.84, 27.52, 29.70, 30.35, 32.48, 116.50 (2C), 118.35, 118.82, 126.25, 128.42 (2C), 129.27, 132.80, 133.02, 157.49, 158.32, 163.25. HPLC analysis (method A): retention time = 13.428 min; peak area, 99% (254 nm). Elemental analysis for $C_{20}H_{25}NO_3$ calculated: % C, 73.37; % H, 7.70; % N, 4.28; found: % C, 73.40; % H, 7.69; % N, 4.28.

(*E*)-1-(4-hydroxy-4'-methoxy-[1,1'-biphenyl]-3-yl)octan-1-one oxime (**11d**). White solid, yield: 74% from **33** (eluent: *n*-hexane/EtOAc 9:1). ^{1}H-NMR (acetone-d_6) δ (ppm): 0.87 (t, 3H, J = 7.0 Hz), 1.24-1.43 (m, 6H), 1.48 (quint, 2H, J = 7.3 Hz), 1.68 (quint, 2H, J = 7.6 Hz), 3.02 (t, 2H, J = 7.9 Hz), 3.83 (s, 3H), 6.95 (d, 1H, J = 8.5 Hz), 7.00 (AA'XX', 2H, J_{AX} = 8.9 Hz, $J_{AA'/XX'}$ = 2.6 Hz), 7.49 (dd, 1H, J = 8.5, 2.2 Hz), 7.54 (AA'XX', 2H, J_{AX} = 8.9 Hz, $J_{AA'/XX'}$ = 2.6 Hz), 7.71 (d, 1H, J = 2.2 Hz), 10.67 (exchangeable s, 1H), 11.58 (exchangeable s, 1H). ^{13}C-NMR (acetone-d_6) δ (ppm): 14.34, 23.30, 24.85, 27.53, 29.71, 30.37, 32.49, 55.59, 115.09 (2C), 118.43, 118.89, 126.41, 128.36 (2C), 129.38, 132.50, 134.06, 158.51, 159.86, 163.23. HPLC analysis (method A): retention time = 16.154 min; peak area, 99% (254 nm). Elemental analysis for $C_{21}H_{27}NO_3$ calculated: % C, 73.87; % H, 7.97; % N, 4.10; found: % C, 73.81; % H, 7.96; % N, 4.09.

(*E*)-1-(3'-fluoro-4,4'-dihydroxy-[1,1'-biphenyl]-3-yl)decan-1-one oxime (**12a**). Light-yellow solid, yield: 91% from **50** (eluent: *n*-hexane/EtOAc 9:1). ^{1}H-NMR (acetone-d_6) δ (ppm): 0.86 (t, 3H, J = 6.9 Hz), 1.17-1.46 (m, 10H), 1.49 (quint, 2H, J = 7.6 Hz), 1.68 (quint, 2H, J = 7.6 Hz), 3.03 (t, 2H, J

= 7.9 Hz), 6.95 (d, 1H, *J* = 8.5 Hz), 7.05 (dd, 1H, *J* = 9.1, 8.5 Hz), 7.29 (ddd, 1H, *J* = 8.4, 2.3, 1.0 Hz), 7.38 (dd, 1H, *J* = 12.6, 2.2 Hz), 7.50 (dd, 1H, *J* = 8.5, 2.3 Hz), 7.73 (d, 1H, *J* = 2.3 Hz), 8.66 (exchangeable bs, 1H), 10.69 (exchangeable bs, 1H), 11.63 (exchangeable s, 1H). ^{13}C-NMR (acetone-d_6) δ (ppm): 14.35, 23.30, 24.78, 27.48, 29.89, 30.09, 30.20, 30.34, 32.59, 114.77 (d, *J* = 19.1 Hz), 118.47, 118.93, 118.97 (d, *J* = 3.0 Hz), 123.32 (d, *J* = 3.5 Hz), 126.42, 129.35, 131.54 (d, *J* = 2.2 Hz), 133.97 (d, *J* = 6.3 Hz), 144.68 (d, *J* = 13.1 Hz), 152.57 (d, *J* = 238.9 Hz), 158.76, 163.21. HPLC analysis (method B): retention time = 12.254 min; peak area, 99% (254 nm). Elemental analysis for $C_{22}H_{28}FNO_3$ calculated: % C, 70.75; % H, 7.56; % N, 3.75; found: % C, 70.83; % H, 7.57; % N, 3.76.

(*E*)-1-(3'-fluoro-4-hydroxy-4'-methoxy-[1,1'-biphenyl]-3-yl)decan-1-one oxime (**12b**). White solid, yield: 84% from **34** (eluent: *n*-hexane/EtOAc 9:1). ^{1}H-NMR (acetone-d_6) δ (ppm): 0.86 (t, 3H, *J* = 6.9 Hz), 1.19-1.43 (m, 10H), 1.49 (quint, 2H, *J* = 7.3 Hz), 1.68 (quint, 2H, *J* = 7.6 Hz), 3.04 (t, 2H, *J* = 7.9 Hz), 3.92 (s, 3H), 6.96 (d, 1H, *J* = 8.5 Hz), 7.19 (t, 1H, *J* = 8.9 Hz), 7.36-7.44 (m, 2H), 7.52 (dd, 1H, *J* = 8.4, 2.3 Hz), 7.75 (d, 1H, *J* = 2.3 Hz), 10.70 (exchangeable s, 1H), 11.65 (exchangeable s, 1H). ^{13}C-NMR (acetone-d_6) δ (ppm): 14.34, 23.31, 24.79, 27.48, 29.89, 30.08, 30.36 (2C), 32.60, 56.57, 114.77 (d, *J* = 19.1 Hz), 114.91 (d, *J* = 2.6 Hz), 118.54, 119.00, 123.10 (d, *J* = 3.7 Hz), 126.55, 129.44, 131.28 (d, *J* = 2.3 Hz), 134.79 (d, *J* = 6.6 Hz), 147.58 (d, *J* = 10.4 Hz), 153.35 (d, *J* = 243.9 Hz), 158.93, 163.21. HPLC analysis (method B): retention time = 15.317 min; peak area, 99% (254 nm). Elemental analysis for $C_{23}H_{30}FNO_3$ calculated: % C, 71.29; % H, 7.80; % N, 3.61; found: % C, 71.23; % H, 7.79; % N, 3.61.

(*E*)-1-(4,4'-dihydroxy-[1,1'-biphenyl]-3-yl)decan-1-one oxime (**12c**). Light-yellow solid, yield: 79% from **51** (eluent: *n*-hexane/EtOAc 85:15). ^{1}H-NMR (acetone-d_6) δ (ppm): 0.87 (t, 3H, *J* = 6.9 Hz), 1.19-1.44 (m, 10H), 1.49 (quint, 2H, *J* = 7.3 Hz), 1.68 (quint, 2H, *J* = 7.7 Hz), 3.02 (t, 2H, *J* = 7.9 Hz), 6.90 (AA'XX', 2H, J_{AX} = 8.8 Hz, $J_{AA'/XX'}$ = 2.6 Hz), 6.93 (d, 1H, *J* = 8.5 Hz), 7.42-7.49 (m, 3H), 7.69 (d, 1H, *J* = 2.2 Hz), 8.37 (exchangeable bs, 1H), 10.66 (exchangeable bs, 1H), 11.55 (exchangeable s, 1H). ^{13}C-NMR (acetone-d_6) δ (ppm): 14.36, 23.31, 24.83, 27.50, 30.01 (2C), 30.20, 30.36, 32.59, 116.49 (2C), 118.35, 118.82, 126.25, 128.42 (2C), 129.27, 132.80, 133.01, 157.48,

158.32, 163.23. HPLC analysis (method B): retention time = 11.959 min; peak area, 99% (254 nm). Elemental analysis for $C_{22}H_{29}NO_3$ calculated: % C, 74.33; % H, 8.22; % N, 3.94; found: % C, 74.25; % H, 8.23; % N, 3.93.

(*E*)-1-(4-hydroxy-4'-methoxy-[1,1'-biphenyl]-3-yl)decan-1-one oxime (**12d**). White solid, yield: 78% from **35** (eluent: *n*-hexane/EtOAc 9:1). ^{1}H-NMR (acetone-d_6) δ (ppm): 0.86 (t, 3H, J = 6.9 Hz), 1.20-1.43 (m, 10H), 1.49 (quint, 2H, J = 6.9 Hz), 1.69 (quint, 2H, J = 7.6 Hz), 3.02 (t, 2H, J = 7.9 Hz), 3.83 (s, 3H), 6.95 (d, 1H, J = 8.5 Hz), 7.00 (AA'XX', 2H, J_{AX} = 8.9 Hz, $J_{AA'/XX'}$ = 2.6 Hz), 7.49 (dd, 1H, J = 8.5, 2.2 Hz), 7.55 (AA'XX', 2H, J_{AX} = 8.9 Hz, $J_{AA'/XX'}$ = 2.6 Hz), 1.71 (d, 1H, J = 2.3 Hz), 10.67 (exchangeable s, 1H), 11.58 (exchangeable s, 1H). ^{13}C-NMR (acetone-d_6) δ (ppm): 14.35, 23.32, 24.85, 27.51, 30.09, 30.28, 30.37 (2C), 32.61, 55.58, 115.08 (2C), 118.43, 118.89, 126.41, 128.36 (2C), 129.39, 132.49, 134.06, 158.51, 159.85, 163.23. HPLC analysis (method B): retention time = 15.514 min; peak area, 100% (254 nm). Elemental analysis for $C_{23}H_{31}NO_3$ calculated: % C, 74.76; % H, 8.46; % N, 3.79; found: % C, 74.74; % H, 8.47; % N, 3.79.

(*E*)-1-(3'-fluoro-4,4'-dihydroxy-[1,1'-biphenyl]-3-yl)dodecan-1-one oxime (**13a**). Yellow solid, yield: 99% from **52** (eluent: *n*-hexane/EtOAc 8:2). ^{1}H-NMR (acetone-d_6) δ (ppm): 0.86 (t, 3H, J = 6.9 Hz), 1.16-1.43 (m, 14H), 1.48 (quint, 2H, J = 7.2 Hz), 1.68 (quint, 2H, J = 7.6 Hz), 3.03 (t, 2H, J = 7.9 Hz), 6.95 (d, 1H, J = 8.5 Hz), 7.05 (dd, 1H, J = 9.2, 8.4 Hz), 7.29 (ddd, 1H, J = 8.4, 2.3, 1.0 Hz), 7.38 (dd, 1H, J = 12.6, 2.2 Hz), 7.50 (dd, 1H, J = 8.5, 2.3 Hz), 7.73 (d, 1H, J = 2.3 Hz), 8.70 (exchangeable bs, 1H), 10.70 (exchangeable bs, 1H), 11.64 (exchangeable s, 1H). ^{13}C-NMR (acetone-d_6) δ (ppm): 14.34, 23.30, 24.78, 27.48, 29.88, 30.07, 30.23, 30.32 (2C), 30.34, 32.60, 114.76 (d, J = 19.0 Hz), 118.46, 118.94 (d, J = 2.2 Hz), 118.98, 123.31 (d, J = 3.0 Hz), 126.41, 129.34, 131.53 (d, J = 1.4 Hz), 133.97 (d, J = 6.6 Hz), 144.67 (d, J = 13.2 Hz), 152.56 (d, J = 239.9 Hz), 158.75, 163.20. HPLC analysis (method B): retention time = 14.283 min; peak area, 99% (254 nm). Elemental analysis for $C_{24}H_{32}FNO_3$ calculated: % C, 71.79; % H, 8.03; % N, 3.49; found: % C, 71.74; % H, 8.01; % N, 3.49.

(*E*)-1-(3'-fluoro-4-hydroxy-4'-methoxy-[1,1'-biphenyl]-3-yl)dodecan-1-one oxime (**13b**). White solid, yield: 75% from **36** (eluent: *n*-hexane/EtOAc 9:1). ^{1}H-NMR (acetone-d_6) δ (ppm): 0.86 (t, 3H, *J* = 6.9 Hz), 1.19-1.43 (m, 14H), 1.48 (quint, 2H, *J* = 6.8 Hz), 1.68 (quint, 2H, *J* = 7.6 Hz), 3.04 (t, 2H, *J* = 7.9 Hz), 3.92 (s, 3H), 6.96 (d, 1H, *J* = 8.5 Hz), 7.19 (t, 1H, *J* = 8.9 Hz), 7.36-7.45 (m, 2H), 7.52 (dd, 1H, *J* = 8.5, 2.3 Hz), 7.75 (d, 1H, *J* = 2.3 Hz), 10.70 (exchangeable s, 1H), 11.65 (exchangeable s, 1H). ^{13}C-NMR (acetone-d_6) δ (ppm): 14.35, 23.32, 24.80, 27.49, 30.07 (2C), 30.26 (2C), 30.36 (2C), 32.63, 56.57, 114.77 (d, *J* = 18.6 Hz), 114.90 (d, *J* = 2.6 Hz), 118.54, 119.00, 123.10 (d, *J* = 3.0 Hz), 126.55, 129.44, 131.27 (d, *J* = 2.2 Hz), 134.79 (d, *J* = 6.6 Hz), 147.58 (d, *J* = 10.9 Hz), 153.35 (d, *J* = 243.7 Hz), 158.93, 163.21. HPLC analysis (method B): retention time = 16.684 min; peak area, 99% (254 nm). Elemental analysis for $C_{25}H_{34}FNO_3$ calculated: % C, 72.26; % H, 8.25; % N, 3.37; found: % C, 72.34; % H, 8.26; % N, 3.37.

(*E*)-1-(4,4'-dihydroxy-[1,1'-biphenyl]-3-yl)dodecan-1-one oxime (**13c**). Yellow solid, yield: 76% from **53** (eluent: *n*-hexane/EtOAc 8:2). ^{1}H-NMR (acetone-d_6) δ (ppm): 0.87 (t, 3H, *J* = 6.9 Hz), 1.16-1.43 (m, 14H), 1.49 (quint, 2H, *J* = 7.1 Hz), 1.68 (quint, 2H, *J* = 7.7 Hz), 3.02 (t, 2H, *J* = 7.9 Hz), 6.91 (AA'XX', 2H, J_{AX} = 8.8 Hz, $J_{AA'/XX'}$ = 2.6 Hz), 6.93 (d, 1H, *J* = 8.5 Hz), 7.43-7.49 (m, 3H), 7.69 (d, 1H, *J* = 2.2 Hz), 8.39 (exchangeable s, 1H), 10.67 (exchangeable s, 1H), 11.55 (exchangeable s, 1H). ^{13}C-NMR (acetone-d_6) δ (ppm): 14.36, 23.32, 24.84, 27.51, 30.06, 30.24, 30.34, 30.36, 30.37, 30.42, 32.62, 116.50 (2C), 118.35, 118.81, 126.23, 128.41 (2C), 129.27, 132.79, 133.00, 157.48, 158.31, 163.24. HPLC analysis (method B): retention time = 13.925 min; peak area, 99% (254 nm). Elemental analysis for $C_{24}H_{33}NO_3$ calculated: % C, 75.16; % H, 8.67; % N, 3.65; found: % C, 75.26; % H, 8.68; % N, 3.65.

(*E*)-1-(4-hydroxy-4'-methoxy-[1,1'-biphenyl]-3-yl)dodecan-1-one oxime (**13d**). White solid, yield: 75% from **37** (eluent: *n*-hexane/EtOAc 9:1). ^{1}H-NMR (acetone-d_6) δ (ppm): 0.87 (t, 3H, *J* = 6.9 Hz), 1.19-1.43 (m, 14H), 1.49 (quint, 2H, *J* = 7.3 Hz), 1.69 (quint, 2H, *J* = 7.7 Hz), 3.02 (t, 2H, *J* = 7.9 Hz), 3.83 (s, 3H), 6.95 (d, 1H, *J* = 8.5 Hz), 7.00 (AA'XX', 2H, J_{AX} = 8.9 Hz, $J_{AA'/XX'}$ = 2.6 Hz), 7.49 (dd, 1H, *J* = 8.5, 2.3 Hz), 7.55 (AA'XX', 2H, J_{AX} = 8.9 Hz, $J_{AA'/XX'}$ = 2.6 Hz), 7.71 (d, 1H, *J* = 2.2

Hz), 10.67 (exchangeable s, 1H), 11.58 (exchangeable s, 1H). ^{13}C-NMR (acetone-d_6) δ (ppm): 14.36, 23.32, 24.79, 27.47, 29.89, 30.08 (2C), 30.35 (3C), 32.62, 55.54, 115.02 (2C), 118.40, 118.83, 126.36, 128.33 (2C), 129.36, 132.44, 133.98, 158.46, 159.79, 163.18. HPLC analysis (method B): retention time = 16.882 min; peak area, 98% (254 nm). Elemental analysis for $C_{25}H_{35}NO_3$ calculated: % C, 75.53; % H, 8.87; % N, 3.52; found: % C, 75.30; % H, 8.84; % N, 3.51.

(*E*)-1-(3'-fluoro-4,4'-dihydroxy-[1,1'-biphenyl]-3-yl)tetradecan-1-one oxime (**14a**). White solid, yield: 88% from **54** (eluent: *n*-hexane/EtOAc 9:1). ^{1}H-NMR (acetone-d_6) δ (ppm): 0.83-0.92 (m, 3H), 1.22-1.44 (m, 18H), 1.49 (quint, 2H, *J* = 7.4 Hz), 1.71 (quint, 2H, *J* = 7.7 Hz), 3.03 (t, 2H, *J* = 7.9 Hz), 7.95 (d, 1H, *J* = 8.5 Hz), 7.05 (dd, 1H, *J* = 9.2, 8.4 Hz), 7.28 (ddd, 1H, *J* = 8.4, 2.3, 1.0 Hz), 7.37 (dd, 1H, *J* = 12.6, 2.2 Hz), 7.50 (dd, 1H, *J* = 8.5, 2.3 Hz), 7.73 (d, 1H, *J* = 2.2 Hz), 8.64 (exchangeable bs, 1H), 10.68 (exchangeable bs, 1H), 11.62 (exchangeable s, 1H). ^{13}C-NMR (acetone-d_6) δ (ppm): 14.33, 23.31 (2C), 24.81, 27.50, 30.05, 30.07, 30.24, 30.35 (2C), 30.37 (2C), 32.62, 114.78 (d, *J* = 19.1 Hz), 118.48, 118.97, 119.01, 123.32 (d, *J* = 2.9 Hz), 126.43, 129.35, 131.56 (d, *J* = 2.2 Hz), 134.02 (d, *J* = 6.6 Hz), 144.69 (d, *J* = 13.2 Hz), 152.61 (d, *J* = 239.9 Hz), 158.78, 163.23. HPLC analysis (method B): retention time = 15.925 min; peak area, 98% (254 nm). Elemental analysis for $C_{26}H_{36}FNO_3$ calculated: % C, 72.70; % H, 8.45; % N, 3.26; found: % C, 72.56; % H, 8.46; % N, 3.27.

(*E*)-1-(3'-fluoro-4-hydroxy-4'-methoxy-[1,1'-biphenyl]-3-yl)tetradecan-1-one oxime (**14b**). Yellow solid, yield: 83% from **38** (eluent: *n*-hexane/EtOAc 9:1). ^{1}H-NMR (acetone-d_6) δ (ppm): 0.88 (t, 3H, *J* = 6.8 Hz), 1.20-1.44 (m, 18H), 1.49 (quint, 2H, *J* = 7.2 Hz), 1.69 (quint, 2H, *J* = 7.5 Hz), 3.04 (t, 2H, *J* = 7.9 Hz), 3.92 (s, 3H), 6.96 (d, 1H, *J* = 8.5 Hz), 7.19 (t, 1H, *J* = 8.9 Hz), 7.36-7.44 (m, 2H), 7.52 (dd, 1H, *J* = 8.5, 2.3 Hz), 7.75 (d, 1H, *J* = 2.2 Hz), 10.68 (exchangeable s, 1H), 11.64 (exchangeable s, 1H). ^{13}C-NMR (acetone-d_6) δ (ppm): 14.35, 23.32 (2C), 24.81, 27.49, 30.07 (2C), 30.25, 30.36 (2C), 30.38 (2C), 32.63, 56.60, 114.78 (d, *J* = 19.1 Hz), 114.95 (d, *J* = 3.0 Hz), 118.54, 119.02, 123.10 (d, *J* = 4.0 Hz), 126.55, 129.44, 131.29 (d, *J* = 1.0 Hz), 134.82 (d, *J* = 7.0 Hz), 147.60 (d, *J* = 11.1 Hz), 153.37 (d, *J* = 243.5 Hz), 158.94, 163.20. HPLC analysis (method B): retention time

= 17.919 min; peak area, 98% (254 nm). Elemental analysis for $C_{27}H_{38}FNO_3$ calculated: % C, 73.10; % H, 8.63; % N, 3.16; found: % C, 72.99; % H, 8.62; % N, 3.16.

(*E*)-1-(4,4'-dihydroxy-[1,1'-biphenyl]-3-yl)tetradecan-1-one oxime (**14c**). Yellow solid, yield: 85% from **55** (eluent: *n*-hexane/EtOAc 85:15). ^{1}H-NMR (acetone-d_6) δ (ppm): 0.87 (t, 3H, J = 6.8 Hz), 1.23-1.44 (m, 18H), 1.49 (quint, 2H, J = 7.3 Hz), 1.69 (quint, 2H, J = 7.6 Hz), 3.02 (t, 2H, J = 7.9 Hz), 6.91 (AA'XX', 2H, J_{AX} = 8.7 Hz, $J_{AA'/XX'}$ = 2.5 Hz), 6.93 (d, 1H, J = 8.5 Hz), 7.42-7.49 (m, 3H), 7.69 (d, 1H, J = 2.3 Hz), 8.34 (exchangeable s, 1H), 10.63 (exchangeable s, 1H), 11.54 (exchangeable s, 1H). ^{13}C-NMR (acetone-d_6) δ (ppm): 14.36, 23.33 (2C), 24.88, 27.53, 30.07, 30.26, 30.39 (2C), 30.40 (2C), 30.41, 32.64, 116.53 (2C), 118.37, 118.86, 126.26, 128.42 (2C), 129.28, 132.82, 133.05, 157.51, 158.35, 163.26. HPLC analysis (method B): retention time = 15.725 min; peak area, 99% (254 nm). Elemental analysis for $C_{26}H_{37}NO_3$ calculated: % C, 75.87; % H, 9.06; % N, 3.40; found: % C, 75.79; % H, 9.06; % N, 3.40.

(*E*)-1-(4-hydroxy-4'-methoxy-[1,1'-biphenyl]-3-yl)tetradecan-1-one oxime (**14d**). White solid, yield: 86% from **39** (eluent: *n*-hexane/EtOAc 9:1). ^{1}H-NMR (acetone-d_6) δ (ppm): 0.89 (t, 3H, J = 6.9 Hz), 1.20-1.44 (m, 18H), 1.49 (quint, 2H, J = 7.2 Hz), 1.69 (quint, 2H, J = 7.5 Hz), 3.02 (t, 2H, J = 7.9 Hz), 3.83 (s, 3H), 6.95 (d, 1H, J = 8.4 Hz), 7.00 (AA'XX', 2H, J_{AX} = 8.9 Hz, $J_{AA'/XX'}$ = 2.6 Hz), 7.49 (dd, 1H, J = 8.5, 2.2 Hz), 7.55 (AA'XX', 2H, J_{AX} = 8.9 Hz, $J_{AA'/XX'}$ = 2.6 Hz), 7.71 (d, 1H, J = 2.2 Hz), 10.66 (exchangeable s, 1H), 11.57 (exchangeable s, 1H). ^{13}C-NMR (acetone-d_6) δ (ppm): 14.37, 23.34 (2C), 24.89, 27.52, 30.09, 30.28 (2C), 30.41 (2C), 30.43 (2C), 32.65, 55.61, 115.11 (2C), 118.45, 118.93, 126.41, 128.36 (2C), 129.39, 132.51, 134.09, 158.54, 159.88, 163.25. HPLC analysis (method B): retention time = 18.337 min; peak area, 98% (254 nm). Elemental analysis for $C_{27}H_{39}NO_3$ calculated: % C, 76.20; % H, 9.24; % N, 3.29; found: % C, 76.07; % H, 9.21; % N, 3.28.

(*E*)-1-(4-hydroxy-[1,1'-biphenyl]-3-yl)tetradecan-1-one oxime (**14e**). White solid, yield: 72% from **42** (eluent: *n*-hexane/EtOAc 9:1). ^{1}H-NMR (acetone-d_6) δ (ppm): 0.87 (t, 3H, J = 6.9 Hz), 1.22-1.43 (m, 18H), 1.49 (quint, 2H, J = 7.2 Hz), 1.69 (quint, 2H, J = 7.6 Hz), 3.04 (t, 2H, J = 7.9 Hz), 6.98 (d, 1H, J = 8.5 Hz), 7.31 (tt, 1H, J = 7.4, 1.4 Hz), 7.40-7.46 (m, 2H), 7.55 (dd, 1H, J = 8.4, 2.2 Hz), 7.59-

7.65 (m, 2H), 7.78 (d, 1H, *J* = 2.3 Hz), 10.70 (exchangeable s, 1H), 11.66 (exchangeable s, 1H). ^{13}C-NMR (acetone-d_6) δ (ppm): 14.36, 23.33 (2C), 24.83, 27.50, 30.01, 30.08 (2C), 30.09, 30.25, 30.36 (2C), 32.63, 118.53, 118.97, 126.88, 127.33 (2C), 127.52, 129.68 (2C), 129.76, 132.67, 141.57, 159.04, 163.20. HPLC analysis (method B): retention time = 19.449 min; peak area, 98% (254 nm). Elemental analysis for $C_{26}H_{37}NO_2$ calculated: % C, 78.94; % H, 9.43; % N, 3.54; found: % C, 78.80; % H, 9.41; % N, 3.53.

(*E*)-1-(3'-fluoro-4-hydroxy-[1,1'-biphenyl]-3-yl)tetradecan-1-one oxime (**14f**). White solid, yield: 53% from **43** (eluent: *n*-hexane/EtOAc 9:1). ^{1}H-NMR (acetone-d_6) δ (ppm): 0.87 (t, 3H, *J* = 6.9 Hz), 1.22-1.43 (m, 18H), 1.49 (quint, 2H, *J* = 7.3 Hz), 1.69 (quint, 2H, *J* = 7.7 Hz), 3.05 (t, 2H, *J* = 7.9 Hz), 6.99 (d, 1H, *J* = 8.5 Hz), 7.04-7.12 (m, 1H), 7.37-7.42 (m, 1H), 7.44-7.50 (m, 2H), 7.59 (dd, 1H, *J* = 8.5, 2.3 Hz), 7.82 (d, 1H, *J* = 2.3 Hz), 10.74 (exchangeable s, 1H), 11.75 (exchangeable s, 1H). ^{13}C-NMR (acetone-d_6) δ (ppm): 14.35, 23.32 (2C), 24.78, 27.48, 30.07, 30.09, 30.24, 30.28, 30.35, 30.37, 30.38, 32.63, 113.88 (d, *J* = 13.3 Hz), 114.09 (d, *J* = 12.5 Hz), 118.65, 119.08, 123.21 (d, *J* = 2.3 Hz), 127.04, 129.82, 131.26, (d, *J* = 2.7 Hz), 131.46 (d, *J* = 8.3 Hz), 144.07 (d, *J* = 8.1 Hz), 159.53, 163.17, 164.17 (d, *J* = 243.6 Hz). HPLC analysis (method B): retention time = 19.200 min; peak area, 99% (254 nm). Elemental analysis for $C_{26}H_{36}FNO_2$ calculated: % C, 75.51; % H, 8.77; % N, 3.39; found: % C, 75.44; % H, 8.78; % N, 3.39.

(*E*)-1-(3',4-dihydroxy-[1,1'-biphenyl]-3-yl)tetradecan-1-one oxime (**14g**). White solid, yield: 77% from **45** (eluent: *n*-hexane/EtOAc 8:2). ^{1}H-NMR (acetone-d_6) δ (ppm): 0.87 (t, 3H, *J* = 6.9 Hz), 1.20-1.43 (m, 18H), 1.49 (quint, 2H, *J* = 7.2 Hz), 1.69 (quint, 2H, *J* = 7.6 Hz), 3.03 (t, 2H, *J* = 7.9 Hz), 6.77-6.82 (m, 1H), 6.96 (d, 1H, *J* = 8.5 Hz), 7.05-7.11 (m, 2H), 7.25 (t, 1H, *J* = 8.1 Hz), 7.51 (dd, 1H, *J* = 8.4, 2.2 Hz), 7.74 (d, 1H, *J* = 2.2 Hz), 10.69 (exchangeable s, 1H), 11.64 (exchangeable s, 1H). ^{13}C-NMR (acetone-d_6) δ (ppm): 14.35, 23.31, 24.83, 27.51, 30.06 (2C), 30.25 (2C), 30.34 (2C), 30.37, 30.38, 32.62, 114.24, 114.52, 118.41, 118.58, 118.85, 126.80, 129.69, 130.68, 132.71, 143.07, 158.73, 159.01, 163.16. HPLC analysis (method B): retention time = 16.133 min; peak area, 98%

(254 nm). Elemental analysis for $C_{26}H_{37}NO_3$ calculated: % C, 75.87; % H, 9.06; % N, 3.40; found: % C, 75.95; % H, 9.05; % N, 3.39.

(*E*)-1-(3'-fluoro-4,4'-dihydroxy-[1,1'-biphenyl]-3-yl)hexadecan-1-one oxime (**15a**). Yellow solid, yield: 91% from **56** (eluent: *n*-hexane/EtOAc 85:15). ^{1}H-NMR (acetone-d_6) δ (ppm): 0.87 (t, 3H, *J* = 6.9 Hz), 1.23-1.44 (m, 22H), 1.49 (quint, 2H, *J* = 7.2 Hz), 1.69 (quint, 2H, *J* = 7.6 Hz), 3.03 (t, 2H, *J* = 7.9 Hz), 6.95 (d, 1H, *J* = 8.5 Hz), 7.05 (dd, 1H, *J* = 9.1, 8.4 Hz), 7.28 (ddd, 1H, *J* = 8.4, 2.3, 1.0 Hz), 7.37 (dd, 1H, *J* = 12.6, 2.2 Hz), 7.50 (dd, 1H, *J* = 8.5, 2.3 Hz), 7.73 (d, 1H, *J* = 2.3 Hz), 8.62 (exchangeable s, 1H), 10.66 (exchangeable s, 1H), 11.61 (exchangeable s, 1H). ^{13}C-NMR (acetone-d_6) δ (ppm): 14.37, 23.34 (2C), 24.84, 27.52, 30.08, 30.27 (2C), 30.37 (2C), 30.39 (2C), 30.41 (2C), 32.65, 114.78 (d, *J* = 19.1 Hz), 118.50, 119.01 (d, *J* = 4.0 Hz), 119.03, 123.33 (d, *J* = 3.0 Hz), 126.43, 129.36, 131.57 (d, *J* = 2.0 Hz), 134.03 (d, *J* = 7.0 Hz), 144.71 (d, *J* = 13.1 Hz), 152.60 (d, *J* = 240.5 Hz), 158.80, 163.22. HPLC analysis (method B): retention time = 17.243 min; peak area, 99% (254 nm). Elemental analysis for $C_{28}H_{40}FNO_3$ calculated: % C, 73.49; % H, 8.81; % N, 3.06; found: % C, 73.50; % H, 8.80; % N, 3.06.

(*E*)-1-(3'-fluoro-4-hydroxy-4'-methoxy-[1,1'-biphenyl]-3-yl)hexadecan-1-one oxime (**15b**). Light-yellow solid, yield: 76% from **40** (eluent: *n*-hexane/EtOAc 9:1). ^{1}H-NMR (acetone-d_6) δ (ppm): 0.86 (t, 3H, *J* = 6.8 Hz), 1.22-1.43 (m, 22H), 1.49 (quint, 2H, *J* = 7.7 Hz), 1.69 (quint, 2H, *J* = 7.6 Hz), 3.04 (t, 2H, *J* = 7.9 Hz), 3.92 (s, 3H), 6.96 (d, 1H, *J* = 8.5 Hz), 7.19 (t, 1H, *J* = 8.9 Hz), 7.36-7.45 (m, 2H), 7.52 (dd, 1H, *J* = 8.5, 2.3 Hz), 7.75 (d, 1H, *J* = 2.3 Hz), 10.69 (exchangeable s, 1H), 11.65 (exchangeable s, 1H). ^{13}C-NMR (acetone-d_6) δ (ppm): 14.36, 23.33 (2C), 24.84, 27.51, 29.70, 29.90, 30.09, 30.27, 30.28, 30.37 (2C), 30.40 (2C), 32.65, 56.64, 114.80 (d, *J* = 19.1 Hz), 115.00 (d, *J* = 2.5 Hz), 118.56, 119.05, 123.22 (d, *J* = 3.7 Hz), 126.57, 129.45, 131.30 (d, *J* = 1.9 Hz), 134.86 (d, *J* = 6.6 Hz), 147.62 (d, *J* = 11.0 Hz), 153.41 (d, *J* = 244.3 Hz), 158.97, 163.22. HPLC analysis (method B): retention time = 19.712 min; peak area, 99% (254 nm). Elemental analysis for $C_{29}H_{42}FNO_3$ calculated: % C, 73.85; % H, 8.98; % N, 2.97; found: % C, 73.76; % H, 8.99; % N, 2.97.

(*E*)-1-(4,4'-dihydroxy-[1,1'-biphenyl]-3-yl)hexadecan-1-one oxime (**15c**). Yellow solid, yield: 79% from **57** (eluent: *n*-hexane/EtOAc 85:15). ^{1}H-NMR (acetone-d_6) δ (ppm): 0.88 (t, 3H, J = 6.8 Hz), 1.22-1.44 (m, 22H), 1.49 (quint, 2H, J = 7.2 Hz), 1.69 (quint, 2H, J = 7.6 Hz), 3.02 (t, 2H, J = 7.9 Hz), 6.91 (AA'XX', 2H, J_{AX} = 8.8 Hz, $J_{AA'/XX'}$ = 2.5 Hz), 6.93 (d, 1H, J = 8.5 Hz), 7.42-7.49 (m, 3H), 7.69 (d, 1H, J = 2.3 Hz), 8.35 (exchangeable s, 1H), 10.64 (exchangeable s, 1H), 11.54 (exchangeable s, 1H). ^{13}C-NMR (acetone-d_6) δ (ppm): 14.36, 23.32 (2C), 24.87, 27.52, 30.07 (2C), 30.25, 30.36, 30.38, 30.40 (4C), 32.63, 116.52 (2C), 118.35, 118.84, 126.24, 128.41 (2C), 129.26, 132.80, 133.03, 157.49, 158.33, 163.23. HPLC analysis (method B): retention time = 17.204 min; peak area, 99% (254 nm). Elemental analysis for $C_{28}H_{41}NO_3$ calculated: % C, 76.50; % H, 9.40; % N, 3.19; found: % C, 76.45; % H, 9.41; % N, 3.18.

(*E*)-1-(4-hydroxy-4'-methoxy-[1,1'-biphenyl]-3-yl)hexadecan-1-one oxime (**15d**). Light-yellow solid, yield: 83% from **41** (eluent: *n*-hexane/EtOAc 95:5). ^{1}H-NMR (acetone-d_6) δ (ppm): 0.87 (t, 3H, J = 6.9 Hz), 1.22-1.43 (m, 22H), 1.49 (quint, 2H, J = 7.1 Hz), 1.69 (quint, 2H, J = 7.6 Hz), 3.02 (t, 2H, J = 7.9 Hz), 3.83 (s, 3H), 6.95 (d, 1H, J = 8.5 Hz), 7.00 (AA'XX', 2H, J_{AX} = 8.9 Hz, $J_{AA'/XX'}$ = 2.6 Hz), 7.49 (dd, 1H, J = 8.4, 2.3 Hz), 7.54 (AA'XX', 2H, J_{AX} = 8.9 Hz, $J_{AA'/XX'}$ = 2.6 Hz), 7.71 (d, 1H, J = 2.3 Hz), 10.65 (exchangeable s, 1H), 11.57 (exchangeable s, 1H). ^{13}C-NMR (acetone-d_6) δ (ppm): 14.37, 23.33 (2C), 24.87, 27.51, 30.08 (2C), 30.26 (2C), 30.38 (5C), 32.64, 55.59, 115.09 (2C), 118.43, 118.91, 126.39, 128.35 (2C), 129.37, 132.49, 134.07, 158.52, 159.86, 163.22. HPLC analysis (method B): retention time = 20.733 min; peak area, 99% (254 nm). Elemental analysis for $C_{29}H_{43}NO_3$ calculated: % C, 76.78; % H, 9.55; % N, 3.09; found: % C, 76.65; % H, 9.54; % N, 3.10.

(*E*)-(3'-fluoro-4,4'-dihydroxy-[1,1'-biphenyl]-3-yl)(phenyl)methanone oxime (**16a**). Yellow solid, yield: 42% from **66** (eluent: *n*-hexane/EtOAc 8:2). ^{1}H-NMR (acetone-d_6) δ (ppm): 6.95 (t, 1H, J = 8.6 Hz), 6.99-7.04 (m, 3H), 7.10 (dd, 1H, J = 12.6, 2.1 Hz), 7.40-7.45 (m, 2H), 7.48-7.60 (m, 4H), 8.62 (exchangeable bs, 1H), 10.71 (exchangeable bs, 1H), 11.33 (exchangeable s, 1H). ^{13}C-NMR (acetone-d_6) δ (ppm): 114.48 (d, J = 19.1 Hz), 118.27, 119.00 (d, J = 3.0 Hz), 120.16, 123.07 (d, J = 2.9 Hz), 128.91, 129.25 (2C), 129.55, 129.59 (2C), 129.84, 131.40 (d, J = 2.3 Hz), 132.72, 133.69 (d,

J = 5.8 Hz), 144.68 (d, *J* = 13.2 Hz), 152.47 (d, *J* = 240.0 Hz), 158.60, 161.46. HPLC analysis (method A): retention time = 11.861 min; peak area, 98% (254 nm). Elemental analysis for $C_{19}H_{14}FNO_3$ calculated: % C, 70.58; % H, 4.36; % N, 4.33; found: % C, 70.48; % H, 4.35; % N, 4.32.

(*E*)-(3'-fluoro-4-hydroxy-4'-methoxy-[1,1'-biphenyl]-3-yl)(phenyl)methanone oxime (**16b**). Yellow solid, yield: 40% from **62** (eluent: *n*-hexane/EtOAc 85:15). ^{1}H-NMR (acetone-d_6) δ (ppm): 3.86 (s, 3H), 7.00-7.05 (m, 2H), 7.07-7.15 (m, 3H), 7.40-7.45 (m, 2H), 7.49-7.60 (m, 4H), 10.72 (exchangeable s, 1H), 11.35 (exchangeable s, 1H). ^{13}C-NMR (acetone-d_6) δ (ppm): 56.52, 114.45 (d, *J* = 19.1 Hz), 114.94 (d, *J* = 2.2 Hz), 118.32, 120.21, 122.85 (d, *J* = 3.0 Hz), 129.03, 129.26 (2C), 129.60 (2C), 129.61, 129.86, 131.14 (d, *J* = 2.2 Hz), 132.70, 134.46 (d, *J* = 6.5 Hz), 147.60 (d, *J* = 11.0 Hz), 153.22 (d, *J* = 244.4 Hz), 158.76, 161.42. HPLC analysis (method A): retention time = 13.154 min; peak area, 97% (254 nm). Elemental analysis for $C_{20}H_{16}FNO_3$ calculated: % C, 71.21; % H, 4.78; % N, 4.15; found: % C, 71.10; % H, 4.79; % N, 4.16.

(*E*)-(4,4'-dihydroxy-[1,1'-biphenyl]-3-yl)(phenyl)methanone oxime (**16c**). Brown solid, yield: 69% from **67** (eluent: *n*-hexane/EtOAc 8:2). ^{1}H-NMR (acetone-d_6) δ (ppm): 6.80 (AA'XX', 2H, J_{AX} = 8.8 Hz, $J_{AA'/XX'}$ = 2.6 Hz), 6.97-7.02 (m, 2H), 7.18 (AA'XX', 2H, J_{AX} = 8.8 Hz, $J_{AA'/XX'}$ = 2.6 Hz), 7.39-7.59 (m, 6H), 8.34 (exchangeable bs, 1H), 10.69 (exchangeable bs, 1H), 11.27 (exchangeable s, 1H). ^{13}C-NMR (acetone-d_6) δ (ppm): 116.46 (2C), 118.12 (2C), 120.04, 128.15 (2C), 128.79, 129.20, 129.45, 129.57 (2C), 129.76, 132.64, 132.68, 132.84, 157.47, 158.16, 161.56. HPLC analysis (method A): retention time = 11.612 min; peak area, 97% (254 nm). Elemental analysis for $C_{19}H_{15}NO_3$ calculated: % C, 74.74; % H, 4.95; % N, 4.59; found: % C, 74.97; % H, 4.96; % N, 4.60.

(*E*)-(4-hydroxy-4'-methoxy-[1,1'-biphenyl]-3-yl)(phenyl)methanone oxime (**16d**). Brown solid, yield: 63% from **63** (eluent: *n*-hexane/EtOAc 85:15). ^{1}H-NMR (acetone-d_6) δ (ppm): 3.77 (s, 3H), 6.89 (AA'XX', 2H, J_{AX} = 8.9 Hz, $J_{AA'/XX'}$ = 2.6 Hz), 6.98-7.03 (m, 2H), 7.27 (AA'XX', 2H, J_{AX} = 8.9 Hz, $J_{AA'/XX'}$ = 2.6 Hz), 7.39-7.44 (m, 2H), 7.47-7.59 (m, 4H), 10.71 (exchangeable s, 1H), 11.30 (exchangeable s, 1H). ^{13}C-NMR (acetone-d_6) δ (ppm): 55.51, 115.03 (2C), 118.18 (2C), 120.10, 128.07 (2C), 128.93, 129.21, 129.54, 129.57 (2C), 129.78, 132.32, 132.80, 133.70, 158.33, 159.80,

161.53. HPLC analysis (method A): retention time = 13.134 min; peak area, 96% (254 nm). Elemental analysis for $C_{20}H_{17}NO_3$ calculated: % C, 75.22; % H, 5.37; % N, 4.39; found: % C, 74.93; % H, 5.35; % N, 4.38.

(*E*)-1-(3'-fluoro-4,4'-dihydroxy-[1,1'-biphenyl]-3-yl)-2-phenylethanone oxime (**17a**). Off-white solid, yield: 96% from **68** (eluent: *n*-hexane/EtOAc 8:2). ^{1}H-NMR (acetone-d_6) δ (ppm): 4.49 (s, 2H), 6.93 (d, 1H, *J* = 9.1 Hz), 7.01 (dd, 1H, *J* = 9.1, 8.3 Hz), 7.16 (ddd, 1H, *J* = 8.4, 2.2, 1.0 Hz), 7.18-7.26 (m, 2H), 7.28-7.34 (m, 2H), 7.38-7.43 (m, 2H), 7.46 (dd, 1H, *J* = 8.5, 2.3 Hz), 7.75 (d, 1H, *J* = 2.2 Hz), 8.61 (exchangeable d, 1H, *J* = 1.6 Hz), 11.01 (exchangeable s, 1H), 11.50 (exchangeable s, 1H). ^{13}C-NMR (acetone-d_6) δ (ppm): 30.71, 114.60 (d, *J* = 19.1 Hz), 118.40, 118.89, 118.92 (d, *J* = 3.4 Hz), 123.14 (d, *J* = 3.1 Hz), 127.14, 127.24, 129.28, 129.33 (3C), 129.52, 131.39 (d, *J* = 2.3 Hz), 133.75 (d, *J* = 5.8 Hz), 137.91, 144.63 (d, *J* = 13.2 Hz), 152.53 (d, *J* = 239.8 Hz), 158.65, 161.05. HPLC analysis (method A): retention time = 12.126 min; peak area, 98% (254 nm). Elemental analysis for $C_{20}H_{16}FNO_3$ calculated: % C, 71.21; % H, 4.78; % N, 4.15; found: % C, 71.20; % H, 4.78; % N, 4.14.

(*E*)-1-(3'-fluoro-4-hydroxy-4'-methoxy-[1,1'-biphenyl]-3-yl)-2-phenylethanone oxime (**17b**). Light-yellow solid, yield: 93% from **64** (eluent: *n*-hexane/EtOAc 9:1). ^{1}H-NMR (acetone-d_6) δ (ppm): 3.90 (s, 3H), 4.49 (s, 2H), 6.94 (d, 1H, *J* = 8.5 Hz), 7.15 (t, 1H, *J* = 8.9 Hz), 7.17-7.22 (m, 1H), 7.23-7.34 (m, 4H), 7.38-7.44 (m, 2H), 7.48 (dd, 1H, *J* = 8.5, 2.3 Hz), 7.77 (d, 1H, *J* = 2.3 Hz), 11.02 (exchangeable s, 1H), 11.53 (exchangeable s, 1H). ^{13}C-NMR (acetone-d_6) δ (ppm): 30.75, 56.58, 114.61 (d, *J* = 19.1 Hz), 114.95 (d, *J* = 2.3 Hz), 118.48, 118.98, 122.93 (d, *J* = 3.7 Hz), 127.28, 129.35 (4C), 129.39, 129.57, 131.14 (d, *J* = 2.1 Hz), 134.59 (d, *J* = 6.6 Hz), 137.93, 147.57 (d, *J* = 11.0 Hz), 153.34 (d, *J* = 244.3 Hz), 158.85, 161.06. HPLC analysis (method A): retention time = 13.365 min; peak area, 98% (254 nm). Elemental analysis for $C_{21}H_{18}FNO_3$ calculated: % C, 71.78; % H, 5.16; % N, 3.99; found: % C, 71.91; % H, 5.16; % N, 4.00.

(*E*)-1-(4,4'-dihydroxy-[1,1'-biphenyl]-3-yl)-2-phenylethanone oxime (**17c**). White solid, yield: 94% from **69** (eluent: *n*-hexane/EtOAc 75:25). ^{1}H-NMR (acetone-d_6) δ (ppm): 4.47 (s, 2H), 6.86

(AA'XX', 2H, J_{AX} = 8.8 Hz, $J_{AA'/XX'}$ = 2.6 Hz), 6.92 (d, 1H, *J* = 8.5 Hz), 7.19 (t, 1H, *J* = 7.4 Hz), 7.27-7.35 (m, 4H), 7.37-7.45 (m, 3H), 7.73 (d, 1H, *J* = 2.3 Hz), 8.33 (exchangeable bs, 1H), 10.98 (exchangeable s, 1H), 11.44 (exchangeable s, 1H). ^{13}C-NMR (acetone-d_6) δ (ppm): 30.80, 116.49 (2C), 118.29, 118.82, 127.01, 127.24, 128.29 (2C), 129.24, 129.35 (2C), 129.54 (2C), 132.68, 132.82, 137.94, 157.45, 158.24, 161.16. HPLC analysis (method A): retention time = 11.927 min; peak area, 98% (254 nm). Elemental analysis for $C_{20}H_{17}NO_3$ calculated: % C, 75.22; % H, 5.37; % N, 4.39; found: % C, 75.09; % H, 5.38; % N, 4.39.

(*E*)-1-(4-hydroxy-4'-methoxy-[1,1'-biphenyl]-3-yl)-2-phenylethanone oxime (**17d**). White solid, yield: 92% from **65** (eluent: *n*-hexane/EtOAc 9:1). ^{1}H-NMR (acetone-d_6) δ (ppm): 3.81 (s, 3H), 4.48 (s, 2H), 6.93 (d, 1H, *J* = 8.1 Hz), 6.95 (AA'XX', 2H, J_{AX} = 8.6 Hz, $J_{AA'/XX'}$ = 2.6 Hz), 7.19 (t, 1H, *J* = 7.4 Hz), 7.27-7.34 (m, 2H), 7.38-7.43 (m, 4H), 7.45 (dd, 1H, *J* = 8.5, 2.3 Hz), 7.75 (d, 1H, *J* = 2.3 Hz), 11.01 (exchangeable s, 1H), 11.47 (exchangeable s, 1H). ^{13}C-NMR (acetone-d_6) δ (ppm): 30.79, 55.55, 115.05, 118.36 (2C), 118.87, 127.14, 127.25, 128.20 (2C), 129.34 (4C), 129.54, 132.35, 133.81, 137.93, 158.41, 159.80, 161.12. HPLC analysis (method A): retention time = 13.362 min; peak area, 97% (254 nm). Elemental analysis for $C_{21}H_{19}NO_3$ calculated: % C, 75.66; % H, 5.74; % N, 4.20; found: % C, 75.50; % H, 5.74; % N, 4.21.

(*E*)-1-(3'-fluoro-4,4'-dihydroxy-[1,1'-biphenyl]-3-yl)-2-methylpropan-1-one oxime (**76**). White solid, yield: 39% from **74** (eluent: *n*-hexane/EtOAc 8:2). ^{1}H-NMR (acetone-d_6) δ (ppm): 1.44 (d, 6H, *J* = 7.1 Hz), 3.72 (sept, 1H, *J* = 7.1 Hz), 6.94 (d, 1H, *J* = 8.4 Hz), 7.05 (dd, 1H, *J* = 9.2, 8.4 Hz), 7.27 (ddd, 1H, *J* = 8.4, 2.2, 1.0 Hz), 7.36 (dd, 1H, *J* = 12.6, 2.2 Hz), 7.47 (dd, 1H, *J* = 8.5, 2.3 Hz), 7.73 (d, 1H, *J* = 2.3 Hz), 8.60 (exchangeable bs, 1H), 10.51 (exchangeable bs, 1H), 11.15 (exchangeable s, 1H). ^{13}C-NMR (acetone-d_6) δ (ppm): 19.13 (2C), 28.96, 114.76 (d, *J* = 19.1 Hz), 118.43, 119.02 (d, *J* = 3.4 Hz), 120.23, 123.34 (d, *J* = 2.9 Hz), 126.85, 129.12, 131.42 (d, *J* = 2.0 Hz), 134.10 (d, *J* = 6.3 Hz), 144.66 (d, *J* = 13.2 Hz), 152.63 (d, *J* = 239.9 Hz), 158.20, 165.21. HPLC analysis (method A): retention time = 11.403 min; peak area, 95% (254 nm). Elemental analysis for $C_{16}H_{16}FNO_3$ calculated: % C, 66.43; % H, 5.57; % N, 4.84; found: % C, 66.20; % H, 5.55; % N, 4.85.

(*E*)-1-(4,4'-dihydroxy-[1,1'-biphenyl]-3-yl)-2-methylpropan-1-one oxime (**77**). White solid, yield: 41% from **75** (eluent: *n*-hexane/EtOAc 85:15). ^{1}H-NMR (acetone-d_6) δ (ppm): 1.44 (d, 6H, J = 7.0 Hz), 3.27 (sept, 1H, J = 7.0 Hz), 6.95 (AA'XX', 2H, J_{AX} = 8.8 Hz, $J_{AA'/XX'}$ = 2.6 Hz), 7.53 (AA'XX', 2H, J_{AX} = 8.6 Hz, $J_{AA'/XX'}$ = 2.5 Hz), 7.54 (dd, 1H, J = 8.5, 1.8 Hz), 7.59 (dd, 1H, J = 8.5, 0.7 Hz), 7.79 (dd, 1H, J = 1.8, 0.7 Hz), 8.42 (exchangeable s, 1H). ^{13}C-NMR (acetone-d_6) δ (ppm): 20.56 (2C), 29.55, 111.09, 116.55, 117.98, 124.24 (2C), 129.21 (2C), 133.27, 138.74, 143.16, 150.80, 157.86, 172.44. HPLC analysis (method A): retention time = 11.952 min; peak area, 99% (254 nm). Elemental analysis for $C_{16}H_{17}NO_3$ calculated: % C, 70.83; % H, 6.32; % N, 5.16; found: % C, 70.90; % H, 6.32; % N, 5.15.

4.2. Biological assays

4.2.1. MAGL inhibition assay. Human recombinant MAGL, and 4-nitrophenylacetate substrate (4-NPA) were purchased from Cayman Chemical. The IC_{50} values for compounds were generated in 96-well microtiter plates. The MAGL reaction was conducted at room temperature at a final volume of 200 µL in 10 mM Tris buffer, pH 7.2, containing 1 mM EDTA. A total of 150 µL of 4-NPA 133.3 µM (final concentration = 100 µM) was added to 10 µL of DMSO containing the appropriate amount of compound. The reaction was initiated by the addition of 40 µL of MAGL (11 ng/well) in such a way that the assay was linear over 30 min. The final concentration of the analyzed compounds ranged from 200 to 0.0128 µM. After the reaction had proceeded for 30 min, absorbance values were then measured by using a VictorX3 PerkinElmer instrument at 405 nm. Two reactions were also run: one reaction containing no compounds and the second one containing neither inhibitor nor enzyme. IC_{50} values were derived from experimental data using the Sigmoidal dose–response fitting of GraphPad Prism software. To remove possible false positive results, for each compound concentration a blank analysis was carried out, and the final absorbance results were obtained detracting the absorbance produced by the presence of all components except MAGL in the same conditions.

4.2.2. DTT interference assay. The inhibition assay was the same described above, with the exception that prior to the addition of 40 µL of MAGL (11 ng/well), the compound-substrate mixture was incubated 15 min in the presence of DTT at a 10 µM concentration [31].

4.2.3. MAGL dilution assay. The enzyme (880 ng in 75 µL of Tris buffer, pH 7.2) was incubated during 60 min at room temperature with 5 µL of compound **14a** (concentration of 20 µM in the mixture) dissolved in DMSO. The MAGL-inhibitor mixture was then diluted 40-fold with the buffer. After 15 min of incubation, the reaction was initiated on a 160 µL aliquot by the addition of 40 µL of 4-NPA 500 µM and the enzyme activity was measured according to the procedure described above.

4.2.4. MAGL preincubation assay. The MAGL reaction was conducted at room temperature at a final volume of 200 µL in 10 mM Tris buffer, pH 7.2, containing 1 mM EDTA. A total of 150 µL of MAGL (11 ng/well) was added to 10 µL of DMSO containing the appropriate amount of compound. After 0 min, 30 min, and 60 min of incubation time the reaction was initiated by the addition of 40 µL of 4-NPA 500 µM. The enzyme activity was then measured according to the procedure described above [32].

4.2.5. FAAH and ABHDs inhibition assays. FAAH, MAGL and ABHDs activity assays were performed as previously described [33]. Briefly, FAAH activity assays were performed using U937 cell homogenate (100 µg) which were diluted in 200 µL of Tris–HCl 10 mM, EDTA 1 mM, pH 8 containing 0.1% fatty acid-free BSA. Compounds were added at the screening concentration of 10 µM and incubated for 30 min at 37 °C. Then, 100 nM of AEA containing 1 nM of [ethanolamine-1-^{3}H]AEA as a tracer was added to the homogenates and incubated for 15 min at 37 °C. The reaction was stopped by the addition of 400 µL of ice-cold $CHCl_3$:MeOH (1:1), samples were vortexed and rapidly centrifuged at 16000 x g for 10 min. at 4 °C. The aqueous phases were collected and the radioactivity was measured for tritium content by liquid scintillation spectroscopy. The *h*ABHD6 and *h*ABHD12 activity was determined using cell homogenates from *h*ABHD6 and *h*ABHD12 stably transfected HEK293 cells. Compound was pre-incubated with 40 µg of cell homogenate for 30 min

at 37 °C in assay buffer (Tris 1 mM, EDTA 10 mM plus 0.1% BSA, pH= 7.6). DMSO was used as vehicle control and WWL70 10 μM or THL 20 μM as positive controls. Then, 10 μM of 2-OG was added and incubated for 5 min at 37 ºC. The reaction was stopped by the addition of 400 μL of ice-cold $CHCl_3$:MeOH (1:1). The samples were vortexed and centrifuged (16000 x g, 10 min, 4 ºC). Aliquots (200 μL) of the aqueous phase were assayed for tritium content by liquid scintillation spectroscopy. Blank values were recovered from tubes containing no enzyme. Basal 2-OG hydrolysis occurring in non-transfected HEK293 cells was subtracted.

4.2.6. CB1 and CB2 receptor binding assays. Receptor binding experiments were performed with membrane preparations as previously reported [34]. Briefly, clean membranes expressing hCB_1 or hCB_2 were re-suspended in binding buffer (50 mM Tris-HCl, 2.5 mM EDTA, 5 mM $MgCl_2$, 0.5% fatty acid-free bovine serum albumin (BSA), pH 7.4) and incubated with vehicle or compounds and 0.5 nM of [^{3}H]CP55,940 for 90 min at 30 °C. Non-specific binding was determined in the presence of 10 μM of WIN55,512. After incubation, membranes were filtered through a pre-soaked 96-well microplate bonded with GF/B filters under vacuum and washed twelve times with 150 μL of ice-cold binding buffer. The radioactivity was measured and the results expressed as [^{3}H]CP55,940 binding.

4.2.7. Relative Binding Affinity assay. Relative binding affinities were determined by competitive radiometric binding assays with 2 nM [^{3}H]estradiol as tracer, as a modification of methods previously described [25,26]. The source of ER was purified full-length human ERα and ERβ purchased from Pan Vera/Invitrogen (Carlsbad, CA). Incubations were done at 0 °C for 18−24 h, and hydroxyapatite was used to absorb the purified receptor−ligand complexes (human ERs) [26]. The binding affinities are expressed as relative binding affinity (RBA) values, where the RBA of estradiol is 100%; under these conditions, the K_d of estradiol for ERα is ~0.2 nM, and for ERβ it is 0.5 nM. The determination of these RBA values is reproducible in separate experiments with a CV of 0.3.

4.2.8. Cell viability assay. Human breast MDA-MB-231, colorectal HCT116 and ovarian CAOV3, OVCAR3 and SKOV3 cancer cells (from ATCC) were maintained at 37 °C in a humidified atmosphere containing 5% CO_2 according to the supplier. Cells (5×10^2) were plated in 96-well

culture plates. The day after seeding, vehicle or compounds were added at different concentrations to the medium. Compounds were added to the cell culture at a concentration ranging from 200 to 0.02 μM. Cell viability was measured after 96 h according to the supplier (Promega, G7571) with a Tecan M1000 instrument. IC_{50} values were calculated from logistical dose response curves. Averages were obtained from triplicates, and error bars are standard deviations.

4.3. Molecular modeling

*4.3.1. Docking of compound **14a**.* The crystal structure of *h*MAGL (pdb code 3PE6 [35]) was taken from the Protein Data Bank [36]. After adding hydrogen atoms, the protein complexed with its reference inhibitor was minimized using Amber14 software [37] and ff14SB force field at 300 K. The complex was placed in a rectangular parallelepiped water box, an explicit solvent model for water, TIP3P, was used and the complex was solvated with a 10 Å water cap. Sodium ions were added as counter-ions to neutralize the system. Two steps of minimization were then carried out; in the first stage, we kept the protein fixed with a position restraint of 500 kcal/mol $Å^2$ and we solely minimized the positions of the water molecules. In the second stage, we minimized the entire system through 5000 steps of steepest descent followed by conjugate gradient (CG) until a convergence of 0.05 kcal/Å•mol. The ligand was built using Maestro [38] and was minimized by means of Macromodel [39] in a water environment using the CG method until a convergence value of 0.05 kcal/Å mol, using the MMFFs force field and a distance-dependent dielectric constant of 1.0. Automated docking was carried out by means of the AUTODOCK 4.2 program [40]; Autodock Tools [41] was used in order to identify the torsion angles in the ligands, add the solvent model and assign the Kollman atomic charges to the protein. The ligand charge was calculated using the Gasteiger method. The regions of interest used by Autodock were defined by considering the ZYH reference inhibitor as the central group; in particular, a grid of 82, 40, and 30 points in the x, y, and z directions centered on the center of the mass of this compound was constructed. A grid spacing of 0.375 Å and a distance-dependent function of the dielectric constant were used for the energetic map calculations. Using the Lamarckian

Genetic Algorithm, the docked compound were subjected to 200 runs of the AUTODOCK search as previously described [42].

4.3.2. MD Simulations. All simulations were performed using AMBER, version 14 [37]. MD simulations were carried out using the ff14SB force field at 300 K. The complex was placed in a rectangular parallelepiped water box. An explicit solvent model for water, TIP3P, was used, and the complex was solvated with a 20 Å water cap. Sodium ions were added as counterions to neutralize the system. Prior to MD simulations, two steps of minimization were carried out using the same procedure described above. Particle mesh Ewald (PME) electrostatics and periodic boundary conditions were used in the simulation [43]. The MD trajectory was run using the minimized structure as the starting conformation. The time step of the simulations was 2.0 fs with a cutoff of 10 Å for the nonbonded interactions, and SHAKE was employed to keep all bonds involving hydrogen atoms rigid. Constant-volume periodic boundary MD was carried out for 1.0 ns, during which the temperature was raised from 0 to 300 K. Then 99 ns of constant pressure periodic boundary MD was carried out at 300 K using the Langevin thermostat to maintain constant the temperature of our system. All the α carbons of the protein were blocked with a harmonic force constant of 10 kcal/mol•$Å^2$. General Amber force field (GAFF) parameters were assigned to the ligand, while partial charges were calculated using the AM1-BCC method as implemented in the Antechamber suite of AMBER 14. The final structure of the complex was obtained as the average of the last 5.0 ns of MD minimized by the CG method until a convergence of 0.05 kcal/mol•$Å^2$. The average structure was obtained using the Cpptraj program [44] implemented in AMBER 14.

Acknowledgments

We are grateful to the University of Pisa (Progetti di Ricerca di Ateneo, prog. n. PRA-2017-51 and PRA-2018-18) and the National Institutes of Health (PHS 5R01015556 to J.A.K.) for funding. A. Chicca thanks Prof. Juerg Gertsch (Institute of Biochemistry and Molecular Medicine, University of Bern, Switzerland) for the valuable support to perform experiments and for inspiring discussions.

References

[1] J.L. Blankman, B.F. Cravatt, Chemical Probes of Endocannabinoid Metabolism, Pharmacol. Rev. 65 (2013) 849–871. doi:10.1124/pr.112.006387.

[2] D.K. Nomura, D.P. Lombardi, J.W. Chang, S. Niessen, A.M. Ward, J.Z. Long, H.H. Hoover, B.F. Cravatt, Monoacylglycerol lipase exerts dual control over endocannabinoid and fatty acid pathways to support prostate cancer, Chem. Biol. 18 (2011) 846–856. doi:10.1016/j.chembiol.2011.05.009.

[3] L. Ye, B. Zhang, E.G. Seviour, K. xiong Tao, X. hua Liu, Y. Ling, J. ying Chen, G. bin Wang, Monoacylglycerol lipase (MAGL) knockdown inhibits tumor cells growth in colorectal cancer, Cancer Lett. 307 (2011) 6–17. doi:10.1016/j.canlet.2011.03.007.

[4] D.K. Nomura, J.Z. Long, S. Niessen, H.S. Hoover, S.W. Ng, B.F. Cravatt, Monoacylglycerol Lipase Regulates a Fatty Acid Network that Promotes Cancer Pathogenesis, Cell. 140 (2010) 49–61. doi:10.1016/j.cell.2009.11.027.

[5] M.M. Mulvihill, D.K. Nomura, Therapeutic potential of monoacylglycerol lipase inhibitors, Life Sci. 92 (2013) 492–497. doi:10.1016/j.lfs.2012.10.025.

[6] D.K. Nomura, B.E. Morrison, J.L. Blankman, J.Z. Long, S.G. Kinsey, M.C.G. Marcondes, A.M. Ward, Y.K. Hahn, A.H. Lichtman, B. Conti, B.F. Cravatt, Endocannabinoid hydrolysis generates brain prostaglandins that promote neuroinflammation, Science. 334 (2011) 809–813. doi:10.1126/science.1209200.

[7] A. Chicca, J. Marazzi, J. Gertsch, The antinociceptive triterpene β-amyrin inhibits 2-arachidonoylglycerol (2-AG) hydrolysis without directly targeting cannabinoid receptors, Br. J. Pharmacol. 167 (2012) 1596–1608. doi:10.1111/j.1476-5381.2012.02059.x.

[8] J. Guindon, A. Guijarro, D. Piomelli, A.G. Hohmann, Peripheral antinociceptive effects of inhibitors of monoacylglycerol lipase in a rat model of inflammatory pain, Br. J. Pharmacol. 163 (2011) 1464–1478. doi:10.1111/j.1476-5381.2010.01192.x.

[9] J.E. Schlosburg, J.L. Blankman, J.Z. Long, D.K. Nomura, B. Pan, S.G. Kinsey, P.T. Nguyen, D. Ramesh, L. Booker, J.J. Burston, E.A. Thomas, D.E. Selley, L.J. Sim-Selley, Q.S. Liu, A.H. Lichtman, B.F. Cravatt, Chronic monoacylglycerol lipase blockade causes functional antagonism of the endocannabinoid system, Nat. Neurosci. 13 (2010) 1113–1119. doi:10.1038/nn.2616.

[10] L. Scalvini, D. Piomelli, M. Mor, Monoglyceride lipase: Structure and inhibitors, Chem. Phys. Lipids. 197 (2016) 13–24. doi:10.1016/j.chemphyslip.2015.07.011.

[11] J.Z. Long, W. Li, L. Booker, J.J. Burston, S.G. Kinsey, J.E. Schlosburg, F.J. Pavón, A.M. Serrano, D.E. Selley, L.H. Parsons, A.H. Lichtman, B.F. Cravatt, Selective blockade of 2-arachidonoylglycerol hydrolysis produces cannabinoid behavioral effects, Nat. Chem. Biol. 5 (2009) 37–44. doi:10.1038/nchembio.129.

[12] G.G. Muccioli, G. Labar, D.M. Lambert, CAY10499, a novel monoglyceride lipase inhibitor evidenced by an expeditious MGL assay, Chembiochem. 9 (2008) 2704–2710. doi:10.1002/cbic.200800428.

[13] A.R. King, E.Y. Dotsey, A. Lodola, K.M. Jung, A. Ghomian, Y. Qiu, J. Fu, M. Mor, D. Piomelli, Discovery of Potent and Reversible Monoacylglycerol Lipase Inhibitors, Chem.

Biol. 16 (2009) 1045–1052. doi:10.1016/j.chembiol.2009.09.012.

[14] L. Wang, G. Wang, D. Yang, X. Guo, Y. Xu, B. Feng, J. Kang, Euphol arrests breast cancer cells at the G1 phase through the modulation of cyclin D1, p21 and p27 expression, Mol. Med. Rep. 8 (2013) 1279–1285. doi:10.3892/mmr.2013.1650.

[15] G. Hernández-Torres, M. Cipriano, E. Hedén, E. Björklund, A. Canales, D. Zian, A. Feliú, M. Mecha, C. Guaza, C.J. Fowler, S. Ortega-Gutiérrez, M.L. López-Rodríguez, A reversible and selective inhibitor of monoacylglycerol lipase ameliorates multiple sclerosis, Angew. Chemie - Int. Ed. 53 (2014) 13765–13770. doi:10.1002/anie.201407807.

[16] T. Tuccinardi, C. Granchi, F. Rizzolio, I. Caligiuri, V. Battistello, G. Toffoli, F. Minutolo, M. Macchia, A. Martinelli, Identification and characterization of a new reversible MAGL inhibitor, Bioorganic Med. Chem. 22 (2014) 3285–3291. doi:10.1016/j.bmc.2014.04.057.

[17] C. Granchi, F. Rizzolio, S. Palazzolo, S. Carmignani, M. MacChia, G. Saccomanni, C. Manera, A. Martinelli, F. Minutolo, T. Tuccinardi, Structural Optimization of 4-Chlorobenzoylpiperidine Derivatives for the Development of Potent, Reversible, and Selective Monoacylglycerol Lipase (MAGL) Inhibitors, J. Med. Chem. 59 (2016) 10299–10314. doi:10.1021/acs.jmedchem.6b01459.

[18] M. Aghazadeh Tabrizi, P.G. Baraldi, S. Baraldi, E. Ruggiero, L. De Stefano, F. Rizzolio, L. Di Cesare Mannelli, C. Ghelardini, A. Chicca, M. Lapillo, J. Gertsch, C. Manera, M. Macchia, A. Martinelli, C. Granchi, F. Minutolo, T. Tuccinardi, Discovery of 1,5-Diphenylpyrazole-3-Carboxamide Derivatives as Potent, Reversible, and Selective Monoacylglycerol Lipase (MAGL) Inhibitors, J. Med. Chem. 61 (2018) 1340–1354. doi:10.1021/acs.jmedchem.7b01845.

[19] J.Z. Patel, S. Ahenkorah, M. Vaara, M. Staszewski, Y. Adams, T. Laitinen, D. Navia-Paldanius, T. Parkkari, J.R. Savinainen, K. Walczyński, J.T. Laitinen, T.J. Nevalainen, Loratadine analogues as MAGL inhibitors, Bioorg. Med. Chem. Lett. 25 (2015) 1436–1442. doi:10.1016/j.bmcl.2015.02.037.

[20] I. Paterni, S. Bertini, C. Granchi, T. Tuccinardi, M. Macchia, A. Martinelli, I. Caligiuri, G. Toffoli, F. Rizzolio, K.E. Carlson, B.S. Katzenellenbogen, J.A. Katzenellenbogen, F. Minutolo, Highly selective salicylketoxime-based estrogen receptor β agonists display antiproliferative activities in a glioma model, J. Med. Chem. 58 (2015) 1184–1194. doi:10.1021/jm501829f.

[21] N. Miyaura, A. Suzuki, Palladium-catalyzed Cross coupling reactions Organoboron Compounds, Chem. Rev. 95 (1995) 2457–2483. doi:10.1021/ol200371n.

[22] C.N. Kapanda, G.G. Muccioli, G. Labar, J.H. Poupaert, D.M. Lambert, Bis(dialkylaminethiocarbonyl)disulfides as potent and selective monoglyceride lipase inhibitors, J. Med. Chem. 52 (2009) 7310–7314. doi:10.1021/jm901323s.

[23] N. Matuszak, G.G. Muccioli, G. Labar, D.M. Lambert, Synthesis and in vitro evaluation of N-substituted maleimide derivatives as selective monoglyceride lipase inhibitors, J. Med. Chem. 52 (2009) 7410–7420. doi:10.1021/jm900461w.

[24] A.R. King, A. Lodola, C. Carmi, J. Fu, M. Mor, D. Piomelli, A critical cysteine residue in monoacylglycerol lipase is targeted by a new class of isothiazolinone-based enzyme inhibitors, Br. J. Pharmacol. 157 (2009) 974–983. doi:10.1111/j.1476-5381.2009.00276.x.

[25] J.A. Katzenellenbogen, H.J. Johnson, H.N. Myers, Photoaffinity Labels for Estrogen Binding Proteins of Rat Uterus, Biochemistry. 12 (1973) 4085–4092. doi:10.1021/bi00745a010.

[26] K.E. Carlson, I. Choi, A. Gee, B.S. Katzenellenbogen, J.A. Katzenellenbogen, Altered ligand binding properties and enhanced stability of a constitutively active estrogen receptor: Evidence that an open pocket conformation is required for ligand interaction, Biochemistry. 36 (1997) 14897–14905. doi:10.1021/bi971746l.

[27] Y.Y. Wang, C. Attané, D. Milhas, B. Dirat, S. Dauvillier, A. Guerard, J. Gilhodes, I. Lazar, N. Alet, V. Laurent, S. Le Gonidec, D. Biard, C. Hervé, F. Bost, G.S. Ren, F. Bono, G. Escourrou, M. Prentki, L. Nieto, P. Valet, C. Muller, Mammary adipocytes stimulate breast cancer invasion through metabolic remodeling of tumor cells, JCI Insight. 2 (2017) e87489. doi:10.1172/jci.insight.87489.

[28] M. Ma, J. Bai, Y. Ling, W. Chang, G. Xie, R. Li, G. Wang, K. Tao, Monoacylglycerol lipase inhibitor JZL184 regulates apoptosis and migration of colorectal cancer cells, Mol. Med. Rep. 13 (2016) 2850–2856. doi:10.3892/mmr.2016.4829.

[29] A. Daina, O. Michielin, V. Zoete, SwissADME: A free web tool to evaluate pharmacokinetics, drug-likeness and medicinal chemistry friendliness of small molecules, Sci. Rep. 7 (2017) 42717. doi:10.1038/srep42717.

[30] T. Sander, J. Freyss, M. Von Korff, C. Rufener, DataWarrior: An open-source program for chemistry aware data visualization and analysis, J. Chem. Inf. Model. 55 (2015) 460–473. doi:10.1021/ci500588j.

[31] C. Granchi, F. Rizzolio, V. Bordoni, I. Caligiuri, C. Manera, M. Macchia, F. Minutolo, A. Martinelli, A. Giordano, T. Tuccinardi, 4-Aryliden-2-methyloxazol-5(4H)-one as a new scaffold for selective reversible MAGL inhibitors, J. Enzyme Inhib. Med. Chem. 31 (2016) 137–146. doi:10.3109/14756366.2015.1010530.

[32] C. Granchi, I. Caligiuri, E. Bertelli, G. Poli, F. Rizzolio, M. Macchia, A. Martinelli, F. Minutolo, T. Tuccinardi, Development of terphenyl-2-methyloxazol-5(4H)-one derivatives as selective reversible MAGL inhibitors, J. Enzyme Inhib. Med. Chem. 32 (2017) 1240–1252. doi:10.1080/14756366.2017.1375484.

[33] A. Chicca, S. Nicolussi, R. Bartholomäus, M. Blunder, A. Aparisi Rey, V. Petrucci, I. del C. Reynoso-Moreno, J.M. Viveros-Paredes, M. Dalghi Gens, B. Lutz, H.B. Schiöth, M. Soeberdt, C. Abels, R.-P. Charles, K.-H. Altmann, J. Gertsch, Chemical probes to potently and selectively inhibit endocannabinoid cellular reuptake, Proc. Natl. Acad. Sci. 114 (2017) E5006–E5015. doi:10.1073/pnas.1704065114.

[34] A. Chicca, D. Caprioglio, A. Minassi, V. Petrucci, G. Appendino, O. Taglialatela-Scafati, J. Gertsch, Functionalization of beta-caryophyllene generates novel polypharmacology in the endocannabinoid system, ACS Chem. Biol. 9 (2014) 1499–1507. doi:10.1021/cb500177c.

[35] C. Schalk-Hihi, C. Schubert, R. Alexander, S. Bayoumy, J.C. Clemente, I. Deckman, R.L. DesJarlais, K.C. Dzordzorme, C.M. Flores, B. Grasberger, J.K. Kranz, F. Lewandowski, L. Liu, H. Ma, D. Maguire, M.J. Macielag, M.E. McDonnell, T.M. Haarlander, R. Miller, C. Milligan, C. Reynolds, L.C. Kuo, Crystal structure of a soluble form of human monoglyceride lipase in complex with an inhibitor at 1.35 Å resolution, Protein Sci. 20 (2011) 670–683. doi:10.1002/pro.596.

[36] H.M. Berman, The Protein Data Bank, Nucleic Acids Res. 28 (2000) 235–242. doi:10.1093/nar/28.1.235.

[37] R.E. D.A. Case, V. Babin, J.T. Berryman, R.M. Betz, Q. Cai, D.S. Cerutti, T.E. Cheatham, III, T.A. Darden, A.K. Duke, H. Gohlke, A.W. Goetz, S. Gusarov, N. Homeyer, P. Janowski,

J. Kaus, I. Kolossváry, C.S. T.S. Lee, S. LeGrand, T. Luchko, R. Luo, B. Madej, K.M. Merz, F. Paesani, D.R. Roe, A. Roitberg, X. R. Salomon-Ferrer, G. Seabra, C.L. Simmerling, W. Smith, J. Swails, R.C. Walker, J. Wang, R.M. Wolf, W. and P.A. Kollman, AMBER, (2015).

[38] Maestro, (2016).

[39] Macromodel, (2009).

[40] G.M. Morris, D.S. Goodsell, R.S. Halliday, R. Huey, W.E. Hart, R.K. Belew, A.J. Olson, Automated docking using a Lamarckian genetic algorithm and an empirical binding free energy function, J. Comput. Chem. 19 (1998) 1639–1662. doi:10.1002/(SICI)1096-987X(19981115)19:14<1639::AID-JCC10>3.0.CO;2-B.

[41] G.M. Morris, H. Ruth, W. Lindstrom, M.F. Sanner, R.K. Belew, D.S. Goodsell, A.J. Olson, AutoDock4 and AutoDockTools4: Automated docking with selective receptor flexibility, J. Comput. Chem. 30 (2009) 2785–2791. doi:10.1002/jcc.21256.

[42] F. Dal Piaz, M.B. Vera Saltos, S. Franceschelli, G. Forte, S. Marzocco, T. Tuccinardi, G. Poli, S. Nejad Ebrahimi, M. Hamburger, N. De Tommasi, A. Braca, Drug Affinity Responsive Target Stability (DARTS) Identifies Laurifolioside as a New Clathrin Heavy Chain Modulator, J. Nat. Prod. 79 (2016) 2681–2692. doi:10.1021/acs.jnatprod.6b00627.

[43] D.M. York, T.A. Darden, L.G. Pedersen, The effect of long-range electrostatic interactions in simulations of macromolecular crystals: A comparison of the Ewald and truncated list methods, J. Chem. Phys. 99 (1993) 8345–8348. doi:10.1063/1.465608.

[44] D.R. Roe, T.E. Cheatham, PTRAJ and CPPTRAJ: Software for processing and analysis of molecular dynamics trajectory data, J. Chem. Theory Comput. 9 (2013) 3084–3095. doi:10.1021/ct400341p.